

**DEVELOPMENT OF POLYMER COMPOSITES FOR BUILDING MATERIAL  
APPLICATION**

**SIOW KUAI QING**

**A project report submitted in partial fulfilment of the requirements for the award  
of the degree of Bachelor of Engineering (Hons) Petrochemical Engineering**

**Faculty of Engineering and Green Technology**

**Universiti Tunku Abdul Rahman**

**May 2018**

## DECLARATION

I hereby declare that this project report is based on my original work except for citations and quotations which have been duly acknowledged. I also declare that it has not been previously and concurrently submitted for any other degree or award at UTAR or other institutions.

Signature : \_\_\_\_\_

Name : \_\_\_\_\_

ID No. : \_\_\_\_\_

Date : \_\_\_\_\_

**APPROVAL FOR SUBMISSION**

I certify that this project report entitled **“DEVELOPMENT OF POLYMER COMPOSITES FOR BUILDING MATERIAL APPLICATION”** was prepared by **SIOW KUAI QING** has met the required standard for submission in partial fulfilment of the requirements for the award of Bachelor of Engineering (Hons.) Petrochemical Engineering at Universiti Tunku Abdul Rahman.

Approved by,

Signature : \_\_\_\_\_

Supervisor : Dr. Yamuna a/p Munusamy

Date : \_\_\_\_\_

Signature : \_\_\_\_\_

Co-Supervisor : Ir. Dr. Ng Choon Aun

Date : \_\_\_\_\_

The copyright of this report belongs to the author under the terms of the copyright Act 1987 as qualified by Intellectual Property Policy of Universiti Tunku Abdul Rahman. Due acknowledgement shall always be made of the use of any material contained in, or derived from, this report.

© 2018, Siow Kuai Qing. All right reserved

## ACKNOWLEDGEMENTS

I would like to express my outmost gratitude to my research supervisor, Dr. Yamuna Munusamy for her guidance throughout the development of the research. I would also like to thank the lecturers and staffs of UTAR especially Mr Yong Tzyy Jeng, Mr Chin Kah Seng and Ms Mirohsha a/p Mohan who had given me a lot of assistance and advice during the course of the project.

In addition, I would also like to express my gratitude to my loving parent and friends who had helped and given me encouragement throughout the project.

## **DEVELOPMENT OF POLYMER COMPOSITES FOR BUILDING MATERIAL APPLICATION**

### **ABSTRACT**

Construction is one of world's largest polymer composite materials consuming sector. In this study, high density polyethylene (HDPE)-sand composites with high filler loadings was fabricated by using melt blending technique. The composite was characterized and tensile performance was tested. Energy Dispersive X-ray Spectroscopy (EDX) results indicated the elementary component in the sand consisted of Si and O, in the form of silicon dioxide ( $\text{SiO}_2$ ). Particle size analysis (PSA) was carried out to measure the range of sand particle size before melt blending with HDPE. Variety of alkanes and alkenes functional groups were found in the neat HDPE from Fourier Transform Infrared Spectroscopy (FTIR). When the composite filler loading increased to 60wt%, the intensity of functional group for HDPE significantly reduced and the pattern of the functional groups are similar with sand. Melting temperature decreased as filler loading increased while no significant changes was observed on the crystallization temperature for the composites. Which indicates that the processing could be done at lower temperature. The degree of crystallinity for composites at 20wt% sand loading was the highest. Stabilization torque for composites are lower than neat HDPE which mean it was easier to process in melt blending technique. Melt flow index (MFI) results indicated that 20wt% sand loaded composites had the lowest viscosity and easy to flow. Thermal decomposition temperature at 10% decomposition increased  $21^\circ\text{C}$  as filler loading increased up to 60 wt%. The highest value of modulus was achieved at 40 wt% sand loading with increment of 62% compared to neat HDPE which mean it is the stiffest among all. At 60 wt% filler

loading the modulus decreases. Fracture surface of 60wt% filler loaded composites show brittle fracture with apparent voids and poor dispersion of filler in the matrix. The optimum loading for sand filler are between 20wt% to 40wt%.

Keywords: HDPE; Sand; Composite; Thermal Properties; Tensile Properties

**TABLE OF CONTENTS**

<b>DECLARATION</b>	<b>ii</b>
<b>APPROVAL FOR SUBMISSION</b>	<b>iii</b>
<b>ACKNOWLEDGEMENTS</b>	<b>v</b>
<b>ABSTRACT</b>	<b>vi</b>
<b>TABLE OF CONTENTS</b>	<b>viii</b>
<b>LIST OF TABLES</b>	<b>xi</b>
<b>LIST OF FIGURES</b>	<b>xiii</b>
<b>LIST OF SYMBOLS / ABBREVIATIONS</b>	<b>xv</b>
<b>LIST OF APPENDICES</b>	<b>xviii</b>

**CHAPTER**

<b>1</b>	<b>INTRODUCTION</b>	<b>1</b>
	1.1 Background	1
	1.2 Problem Statements	3
	1.3 Research Objectives	5
<b>2</b>	<b>LITERATURE REVIEW</b>	<b>6</b>
	2.1 HDPE	6
	2.2 Sand	10



2.3	Composites	11
2.4	HDPE Composites	16
2.5	Building Materials	21
2.6	Filler	25
<b>3</b>	<b>METHODOLOGY</b>	<b>28</b>
3.1	Materials	28
3.2	Preparation of HDPE-Sand Composite	27
3.3	Characterization	28
3.3.1	Particle Size Analysis (PSA)	28
3.3.2	Morphology Study	29
3.3.3	Fourier Transform Infrared Spectroscopy (FTIR)	29
3.3.4	Thermal Decomposition Study	30
3.3.5	Thermal Properties Analysis	30
3.3.6	Melt Flow Index (MFI)	31
3.3.7	Energy-dispersive X-ray spectroscopy (EDX)	31
3.4	Performance Test	31
3.4.1	Tensile Test	31
3.5	Flow Chart	32
<b>4</b>	<b>RESULTS AND DISCUSSIONS</b>	<b>33</b>
4.1	Characterization of Sand Filler	33
4.1.1	Fourier Transform Infrared Spectroscopy (FTIR)	33
4.1.2	Energy-dispersive X-ray spectroscopy (EDX)	36
4.1.3	Morphology Study	36
4.1.4	Particle Size Analysis	38
4.2	Processing Characteristics of HDPE-Sand Composite	39
4.3	Characterization of HDPE-Sand Composites	41
4.3.1	Fourier Transform Infrared Spectroscopy (FTIR)	41

4.3.2	Thermal Properties of the HDPE-sand composites	43
4.3.3	Melt Flow Index (MFI)	45
4.3.4	Thermal Decomposition Study	46
4.4	Performance Tests of HDPE-Sand Composites	48
4.4.1	Tensile Test	48
<b>5</b>	<b>CONCLUSION AND RECOMMENDATIONS</b>	<b>53</b>
5.1	Conclusion	53
5.2	Recommendation	54
	<b>REFERENCES</b>	<b>55</b>
	<b>APPENDICES</b>	<b>65</b>

**LIST OF TABLES**

<b>TABLE</b>	<b>TITLE</b>	<b>PAGE</b>
Table 1.1:	Tensile properties of HDPE composites	2
Table 2.1:	Physical Properties for LDPE, LLDPE and HDPE	8
Table 2.2:	Mechanical properties of PP and PP-SiO <sub>2</sub> composites, differing in EOC-g-GMA content	13
Table 2.3:	Thermal properties of PP-quartz composites films.	15
Table 2.4:	Thermal properties for HDPE and HDPE with 6 wt% OMMT in as-spun and drawn fibers	20
Table 2.5:	Quantity of plastic waste in the cities of Benin	22
Table 2.6:	Physical and mechanical properties of wood composites plastic and polystyrene	23
Table 2.7:	Summary of physical and mechanical properties of Hybrid Wood-Polypropylene Bio-composite	26
Table 3.1:	Weight of HDPE and Sand for Compounding	28
Table 4.1:	Functional Groups and Absorption Frequency Regions	35
Table 4.2:	Summary of EDX spectrum in wt%	36
Table 4.3:	Functional Groups of HDPE to Peaks in IR Spectra	41

Table 4.4:	DSC results of pure HDPE and composites	44
Table 4.5:	MFI Values of pure HDPE and composites	45
Table 4.6:	Temperature weight loss at 50wt% and 5wt%	47
Table 4.7:	Mechanical Properties of HDPE and HDPE-sand composites	50
Table 4.8:	Comparison of tensile test results	51

## LIST OF FIGURES

<b>FIGURE</b>	<b>TITLE</b>	<b>PAGE</b>
Figure 2.1:	Structure of Polyethylene	8
Figure 2.2:	Polymer Market in 2015	9
Figure 2.3:	SEM image for quartz sand and glass sand.	11
Figure 2.4:	Tensile strength of PP-quartz composites films.	15
Figure 2.5:	Relationship between compressive strength and density of mortar in the dry state	17
Figure 2.6:	TGA curve for a) jute fiber, (b) virgin HDPE, (c) untreated composite, and (d) treated composite.	18
Figure 2.7:	Thermal analysis results of the studied HDPE-mica and HDPE-wollastonite composites	19
Figure 2.8:	Plastic shrinkage cracks on the surfaces of: a) plain concrete, and b), c) and d) FRC with 0.40, 0.75% and 1.25% fibers, respectively with 40× magnification	24
Figure 3.1:	Flow chart of methodology	32
Figure 4.1:	FTIR spectra of sand	34

Figure 4.2:	SEM images of sand at (a) 1000x, (b) 5000x, (c) 10000x and (d) 20000x magnification	37
Figure 4.3:	Particle size distribution for sand	38
Figure 4.4:	Temperature profile for neat HDPE and HDPE-sand composites	39
Figure 4.5:	Stabilization torque for neat HDPE and HDPE-sand composites	40
Figure 4.6:	FTIR spectra for HDPE-sand composites	42
Figure 4.7:	DSC Curves for HDPE-sand composites with different loading	44
Figure 4.8:	TGA curves for HDPE-sand composites	47
Figure 4.9:	Young's Modulus of HDPE-sand composites	49
Figure 4.10:	Tensile strength of HDPE-sand composites	49
Figure 4.11:	Elongation at break of HDPE-sand composites	50
Figure 4.12:	SEM Images of HDPE-sand composites with (a) neat HDPE (b) 20wt% sand (c) 40wt% sand at 3500X and (d) 60wt% sand at 350X	52

**LIST OF SYMBOLS / ABBREVIATIONS**

$\epsilon_{\max}$	Elongation at break
$\sigma_{\max}$	Tensile strength
$\Delta H_m$	Melting heat (J/g)
E	Young's modulus
$T_m$	Melting temperature, °C
$T_c$	Crystallization temperature, °C
$X_c^m$	Degree of crystallinity
ABS	Acrylonitrile butadiene styrene
Al	Aluminium
$Al_2O_3$	Aluminium oxide
ASA	Acrylonitrile styrene acrylate
ATR	Attenuated total reflection
C	Carbon
Ca	Calcium
CFRP	Carbon fiber reinforced polymer

Cu	Copper
DSC	Differential Scanning Calorimetry
EDX	Energy-dispersive X-ray spectroscopy
EOC-g-GMA	Glyceryl methacrylate grafted ethylene/n-octene copolymer
EPS	Expanded Polystyrene
FESEM	Field Emission Scanning Electron Microscopy
FRC	Fiber reinforced concrete
FRP	Fiber reinforced polymer
FRPC	Fiber reinforced polymer composites
FTIR	Fourier Transform Infrared Spectroscopy
GNP	graphite nanoplatelets
HDPE	High density polyethylene
K	Potassium
KBr	Potassium bromide
LCTE	Linear coefficient thermal expansion
LDPE	Low density polyethylene
MA	Myristic acid
MAPE	Maleic Anhydride grafted Polyethylene
MAS	Modular Assembly System
MFI	Melt flow indexer
MFR	Melt flow rate
MMT	Montmorillonite
Mo	Molybdenum



MOE	Modulus of elasticity
MOR	Modulus of rupture
NH <sub>2</sub>	Amide
O	Oxygen
OMMT	Organically modified montmorillonite
PA	Polyamide
PC	Polycarbonate
PET	Polyethylene terephthalate
PMC	Polymer matrix composite
PNC	Polymer nanocomposite
PP	Polypropylene
PS	Polystyrene
PSA	Particle Size Analysis
PUR	Polyurethane
PVC	Poly (vinyl chloride)
RPC	Reinforced polymer composite
SEM	Scanning Electron Microscopy
Si	Silicon
SiO <sub>2</sub>	Silicon dioxide
TGA	Thermal Gravimetric Analysis
UHPC	Ultra-high-performance concrete
UP	Unsaturated polyester
WPCBP	Waste printed circuit boards powders

**LIST OF APPENDICES**

<b>APPENDIXES</b>	<b>TITLE</b>	<b>PAGE</b>
A	Energy-dispersive X-ray spectroscopy	65
B	Fourier Transform Infrared Spectroscopy	66
C	Differential Scanning Calorimetry	69
D	Thermal Gravimetric Analysis	71
E	Particle Size Analysis Report	73

## **CHAPTER 1**

### **INTRODUCTION**

#### **1.1 Background**

High density polyethylene (HDPE) is a linear polymer with superior physical properties than low density polyethylene (LDPE). Thus it can withstand the exposure to variety of solvents and exhibit rigid properties. Addition of filler into HDPE can improve the overall mechanical performance. The fillers are available in wide range such as inorganic or organic fillers, and will exert different properties in HDPE composite (Imai, 2014). Example for organic filler are cellulose, wood powder and coconut fibre while the example for inorganic fillers are silica, talc, calcium carbonate and clay. All these fillers are easy to get and most of them are cheap in cost.

HDPE hits 61.8 billion USD worldwide turnover at 2016 and it is projected to hit 85.8 billion USD turnover by 2022. By now, Asia-pacific countries still the largest customer for the HDPE worldwide and believed to remain the biggest HDPE market in the future (Ceresana, 2015)

The specific modulus and strength of HDPE composite could be elevated to be comparable with other conventional building materials like brick masonry. Young's modulus for brick masonry is 690 MPa (GoBrick, 1992). Young's Modulus for HDPE composite blend with polypropylene (PP) and wood powder in the ratio of 35:35:30 can go as high as 1346 MPa. The mechanical performance of composites with other loadings level are indicated in Table 1.1. From the table it can be observed that the modulus for neat HDPE is only 881 MPa and at the optimum filler loading the stiffness has been increased by 52% (Dikobe and Luyt, 2017). In another research by Sarasini et al, the Young's Modulus for pure HDPE was recorded as 1.1 GPa but upon addition of 40 wt% basalt fibre the value increase up to 6.5 GPa. This shows the promising improvement in mechanical properties for HDPE composites with addition of fillers.

**Table 1.1: Tensile properties of HDPE composites (Dikobe and Luyt, 2017)**

w/w	E/MPa	$\sigma_b$ /MPa	$\epsilon_b$ /%	E/MPa	$\sigma_b$ /MPa	$\epsilon_b$ /MPa
	MAPP/HDPE/WP			PP/HDPE/WP		
100/0/0	472 ± 15	24.9 ± 0.7	13.3 ± 1.2	499 ± 14	29.9 ± 1.3	14.7 ± 2.5
0/100/0	881 ± 37	22.4 ± 1.2	21.9 ± 0.2	881 ± 37	22.4 ± 1.2	21.9 ± 0.2
50/50/0	1128 ± 26	22.8 ± 0.9	19.6 ± 0.3	1060 ± 1	23.1 ± 3.3	6.2 ± 0.4
45/45/10	1140 ± 18	21.7 ± 1.2	10.1 ± 0.3	1204 ± 37	21.6 ± 1.1	3.2 ± 0.3
40/40/20	1143 ± 28	21.4 ± 0.6	7.0 ± 0.3	1340 ± 20	19.0 ± 0.6	2.6 ± 0.2
35/35/30	1156 ± 41	21.5 ± 0.6	5.0 ± 0.1	1346 ± 15	16.1 ± 0.6	2.4 ± 0.2

Construction sector is one of the world's largest polymer composite materials consuming sector (Adarsh, Manikanta and Sha, 2016). In 2016, a Colombia architect, Oscar Méndez used recycle plastics, rubber and electronic wastes to be blended together and become a building block. The building block is "Lego" like and can withstand earthquake and fire retardant. By using the waste and recycle material to prepare the block,

it help to reduce the carbon dioxide emission, energy consumption and as well as lower building cost when compare with traditional building method.

Moulding the bricks into the Lego like shape is possible because of the flexibility and process ability of polymer composite. UK's Poly-Care construction company innovated Modular Assembly System (MAS) which can produce large quantity of bricks enough to build 1200 40m<sup>2</sup> houses with only 60m<sup>2</sup> of factory place. This is due to the whole process for making Lego like bricks are simple and can be performed by an unskilled worker. Brick making machine invented by the company will mix up polyester resin with 90wt% of local sand and the whole process from raw materials preparation to ready use bricks will only take less than 24 hours. This is high efficiency and cost saving as compare with ordinary concrete which may need 2 weeks' time for manufacturing (Mathijsen, 2016).

## **1.2 Problem Statements**

Polymer composite has good potential to be used in the construction sector. Nowadays many constructor apply fiber reinforced polymer (FRP) in construction including bridge, masonry walls, tanks, foundations and buildings. They also applied FRP in repair and rehabilitation of traditional building material. These traditional building material includes concrete, steel, masonry and wood (Mosallam, 2014).

High performance mortar (HPM) can be filled with carbon fiber reinforced polymer (CFRP) to strengthen beam column reinforced concrete joints. The HPM/CFRP composites also use for retrofitted wall and concrete bridge to enhance their performance. By using HPM/CFRP composites, ultimate load of retrofitted wall is increased and improved the bridge collision protection (Mosallam, 2014).

Humphreys (2003) stated that by using reinforced polymer composite (RPC), strength, stiffness, durability, fatigue performance, versatile fabrication of construction material can be improved. Hence these improvement also can lowered down the maintenance cost compare to traditional building materials.

HDPE-sand composite is one of the RPC that have large potential to be applied in construction sector. However in this, initial research the process ability, mechanical properties and thermal durability of the composites had to be evaluated first. This is because sand is a type of coarse and hard particle material. It may cause processing difficulties by affecting the flow ability of the composite melt and may require large energy for melting and mixing. Poor process ability will not only increase the cost of the composite but also will yield poor mechanical properties and low thermal durability. As a replacement for traditional building blocks, it need to be have enough thermal durability against adverse environment and in fire accident. The tensile and stiffness of HDPE-sand composites need to be comparable with other composites in literature.

Thus in this work, HDPE will be mixed with sand composite by using the internal mixer. This method is relatively easy and can be convert to industrial scale. The process ability of the composite will be studied. Overall performance for the HDPE-sand composite film will be tested in terms of mechanical and thermal properties.

### **1.3 Research Objectives**

The aim for this research is to work towards producing Lego like building block by using HDPE-sand composite material with a superior mechanical properties, ease of assembly and price cheaper than traditional building material. However as initial stage, in this work in particular the process ability of this composite and its mechanical and thermal durability properties had been studied. The objectives of the research are:

- i) To produce HDPE-sand composites with high filler loadings by using melt blending technique.
- ii) To evaluate the process ability of the HDPE/Sand composite.
- iii) To test the tensile and thermal decomposition performance of the HDPE-sand composites.

## **CHAPTER 2**

### **LITERATURE REVIEW**

#### **2.1 HDPE**

High density polyethylene (HDPE) is one of the most widely use plastic in the world. HDPE was invented by the Karl Ziegler in 1953 (Professor Plastic, 2015). HDPE is produced by the polymerization of ethylene monomer. HDPE is a type of thermoplastic with density around 0.940 to 0.970 g/cm<sup>3</sup>. The difference between HDPE and low density polyethylene (LDPE) is the crystalline region for HDPE is higher than LDPE. And this will affect the tensile strength and stress crack resistance of the final product (Gabriel, 2010).According to Ryan (2008), HDPE are stiff, tough, can withstand chemical contact and easy to process. Structure of HDPE is as shown in Figure 2.1 (Whisnant, 2000). Some comparison of physical and mechanical properties between linear low density polyethylene (LLDPE), LDPE and HDPE is shown in Table 2.1.



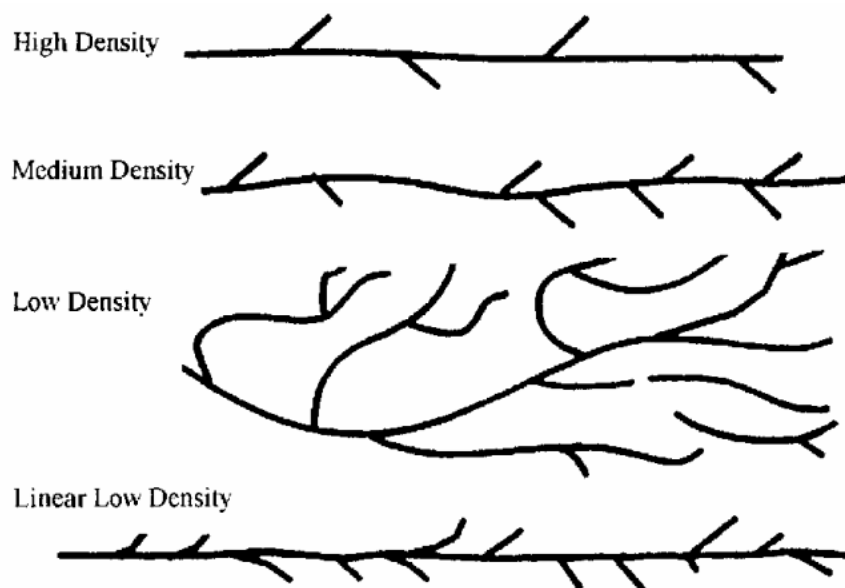


Figure 2.1: Structure of Polyethylene (Kumar Sen and Raut, 2015)

**Table 2.1: Physical Properties for LDPE, LLDPE and HDPE (Kim, Biswas and Choe, 2006)**

<b>Resins (grade name)</b>	<b>Density (g/cm<sup>3</sup>)</b>	<b>MI (g/10 min)</b>	<b>HDT (°C)</b>	<b>Tensile strength (kg/cm<sup>2</sup>)</b>
LDPE (FB 3000)	0.919	3.0	90	120
LLDPE (FT 810)	0.918	2.1	98	350
HDPE (3300)	0.954	0.8	123	30

Wide applications of HDPE lead to high market occupancy worldwide. As 2015, HDPE occupied 15% of total plastics demand in the world as shown in Figure 2.2 (Plastics Europe, 2016).

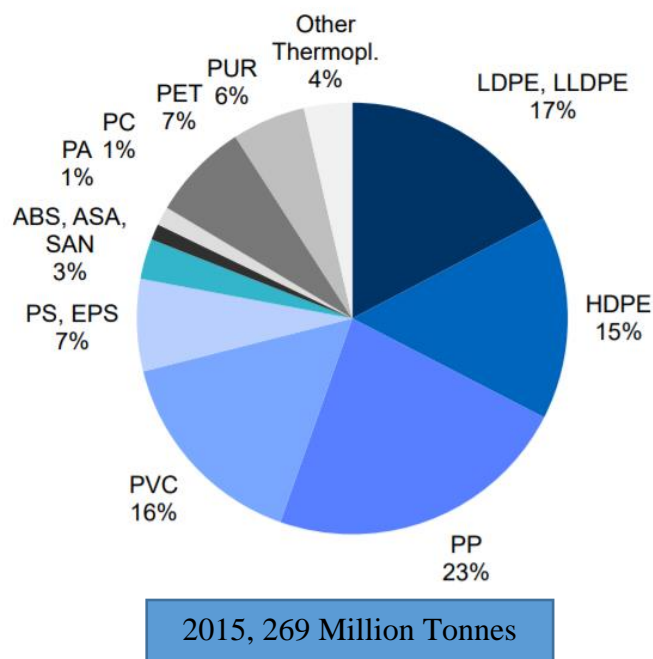


Figure 2.2: Polymer Market in 2015 (Plastics Europe, 2016)

HDPE could perform extremely well at low temperature and exhibit high resistance to abrasion. However, the usage of neat HDPE has been limited because of its low heat distortion and lower modulus (Gao, Liu and Wei, 2011). HDPE can be used to produce heavy duty pipeline for liquid, gas and potable water delivery. According to Zeep Construction (2015), HDPE can be used in heavy duty pipeline because of its flexibility, long service life and durability. It can be bent without using any fitting and this has dramatically reduce the time, cost and labour needed. Hence, in many countries the old pipelines are already replaced with HDPE. The life span of the pipes are longer and thus the cost for maintenance is lower.

In addition, the most common usage of HDPE in our daily life is for packaging purpose. LDPE made film have a relatively clear look and soft feel while HDPE have opaque look and crisp feel. Hence, the HDPE is the most suitable polymer to be used for making food container (Shin and Selke, 2014). In a nutshell, the applications of HDPE

either in industrial or daily life are important. The ease of recycle properties of HDPE also encourage the increase usage of HDPE in innovative green products.

## **2.2 Sand**

Sand is the natural source of mineral that normally could be found at beach, riverbeds and deserts. It comes in loose granular shape that normally made up by silica, silicon dioxide or quartz or calcium carbonate (Castro, 2013). Sand can be classified as pit sand, river sand and sea sand depending on the origin. Beside from the sources, sand with the different grain size will have different usage. Sand with size smaller than 1.5875mm sieve size is classified as fine sand, 3.175mm as coarse sand and 7.62mm as gravelly sand. Fine sands are generally used for plastering, coarse sand used for masonry work and gravelly sand use for concrete work (Patnayaka, 2013). Sand is the major component in building materials like concrete, bricks and plaster due to its stiffness. The bricks made by sand mixed with clay is hard and has greater weight than traditional clay brick (Wang, Ling and Mohri, 2007). Besides, sand is also suitable to act as mineral filler to polymer for building materials application. Figure 2.3 shows the images for glass and quartz sand used as filler in ultra-high performance concrete.

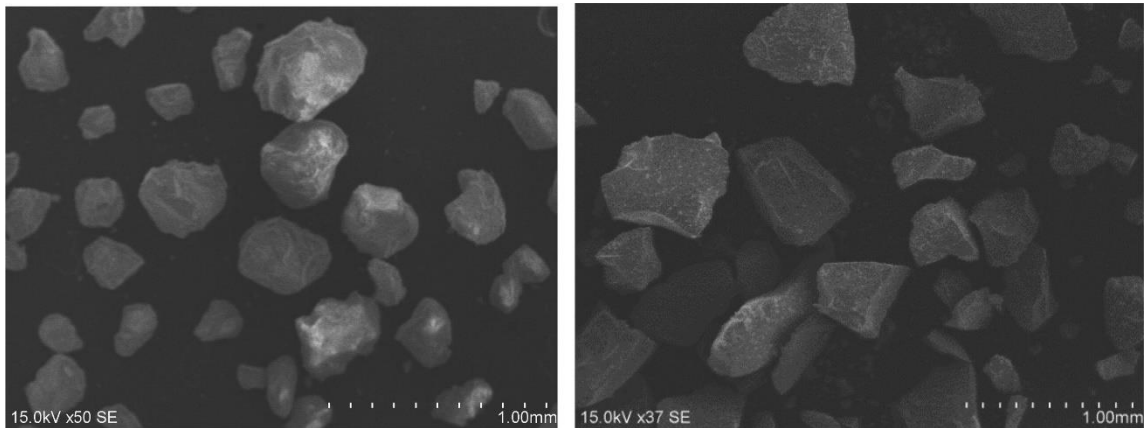


Figure 2.3: SEM image for quartz sand and glass sand (Soliman and Hamou, 2017)

Besides of the high hardness properties, sand also provide bulk strength. Hence, it not only use for concrete and asphalt but also landscaping, sandpaper, glass manufacturing, metal cast moulding and etc. (Chethan, 2016).

### 2.3 Composites

Composite material is made of two types or more constituents, with different properties. The new composite produced will have new properties compared with old material. The composite material can be lighter weight, has high strength and corrosion resistance, show design flexibility, exhibit high-impact strength and dimensional stability (Aly, 2017).

The history of composite that had been used on building can be found around 4000 years ago (Johnson, 2017). Ancient people use mud-straw mixture as composites material to build strong buildings. Ancient people also uses composite mixture in the building as concrete. They mix small stone or gravel together with cement and sand to become

concrete which has good strength than other building material. Researcher also found that ancient people applied the metal rod in the wall of building together with concrete to become reinforced concrete (Wong, 2006). This method still being use until now.

The biggest advantages of composites properties are being light and strong, so it can be used for application that need to operate under harsh environment. Although the price for the composites are higher, in industry it is still chosen because of the design flexibility. By using the suitable matrix and reinforcement material, a new composite that match the properties of traditional material can be form and normally can be moulded into complex shape or pattern (González et al., 2017).

Nowadays, composites materials have widespread use in different field of industry like automotive, construction, manufacturing and also aerospace (CompositesLab, 2016). This show the future possibility of composites because of its good performance when compared with traditional raw materials.

In United States of America, wood fiber-polypropylene composites were widely used in construction sector especially for decking. Alignment of natural fibre in the matrix is an important factor that will affect the tensile, flexural and impact properties of the composite. Aligned fibre in the polymer matrix can achieve an increment in strength up to 70%. In addition, sisal natural fiber is the best performance filler for the composites matrix among other natural fibres such as flax fiber and hemp fiber (Pickering, Efendy and Le, 2016).

Reinforced concrete beam and column that used in building construction also can be bonded with fibre reinforced polymer composites (FRPC) for extra strengthening. The FRPC available in many shape like rod and sheet which are convenient for construction purpose. The polymer matrix can be epoxy, polyester thermosetting plastics or other

thermosets. The FRPC bonded with reinforced concrete beam increased shear strength by 60%-120% compared to pure thermosets. 40% and 200% strength enhancement could be achieved for reinforced concrete beam with glass and carbon fibre respectively (Pendhari, Kant and Desai, 2008). Studzinski et al. (2014) mixed polypropylene (PP) with silica nanoparticles. To enhance the dispersion and compatibility of silica nanoparticles to the PP matrix, glycidyl methacrylate grafted ethylene/n-octene copolymer (EOC-g-GMA) was used as compatibilizer. The mechanical properties for neat PP and composites with different content of compatibilizer are tested and shown in Table 2.2.

**Table 2.2: Mechanical properties of PP and PP-SiO<sub>2</sub> composites, differing in EOC-g-GMA content (Studzinski et al., 2014)**

Property	PP	PP/NH <sub>2</sub> -SiO <sub>2</sub> (98/2)/EOC-g-GMA (wt %)		
		0	4	6
Yield point, MPa	29.5 ± 0.08	28.7 ± 0.16	27.1 ± 0.02	26.3 ± 0.14
Elongation at break, %	53.6 ± 1.4	54.7 ± 1.1	82.1 ± 1.4	95.1 ± 1.0
Tensile modulus, MPa	1250 ± 14	1440 ± 13	1320 ± 10	1275 ± 8
Notched Charpy impact strength, kJ/m <sup>2</sup>	15 ± 0.5	12 ± 0.1	16 ± 0.1	24 ± 0.3

PP-SiO<sub>2</sub> composites tensile modulus increased compared with neat PP, however addition of EOC-g-GMA compatibilizer decreases the modulus. Another significant change for the mechanical properties is elongation at break. PP-SiO<sub>2</sub> composites has higher elongation at break value compared to neat PP and it increased further by adding in the compatibilizer. The dispersion of filler in polymer matrix which is influenced by the compatibilizer significantly affect the properties of the composites.

Phosphogypsum is the by-product from phosphate fertilizer industry. It is not suitable for building construction material usage because of the high density and low flexural strength. To overcome this problem, Verbeek and Plessis (2005) mix the phosphogypsum and phenol formaldehyde resin to gain a useful product. By increasing the content of resin to be more than 50 wt% and the content of coarse phosphogypsum filler to be around 25 wt%, a low density and high strength composite could be formed. With the combination, the strength increased 40% and density decreased 10% compared to pure phosphogypsum.

Unsaturated polyester (UP) always act as the composite matrix for fiber and concrete because of the high performance and low cost. Jo, Park and Kim (2008) made the montmorillonite (MMT)-UP composite and test the mechanical properties and thermal properties of the composite. The results indicate that with 5wt% of nano-MMT filler loading, the tensile strength, Young's modulus and glass transition value are optimum which caused by the good dispersion of filler to UP matrix.

PP based composite reinforced with quartz and extrude to film was researched by Pérez et al. (2015). Filler loadings of quartz are 1wt%, 2.5wt% and 5wt% respectively. The thermal properties of composites were shown in Table 2.3 and tensile strength test result was shown as Figure 2.4.

**Table 2.3: Thermal properties of PP-quartz composites films (Pérez et al., 2015)**

Films	$T_c$ (°C)	$T_f$ (°C)	$X_c$ (%)
PP	116.6	162.1	42
PP-1	119.5	161.2	48
PP-2.5	120.7	160.3	48
PP-5	120.6	161.7	43

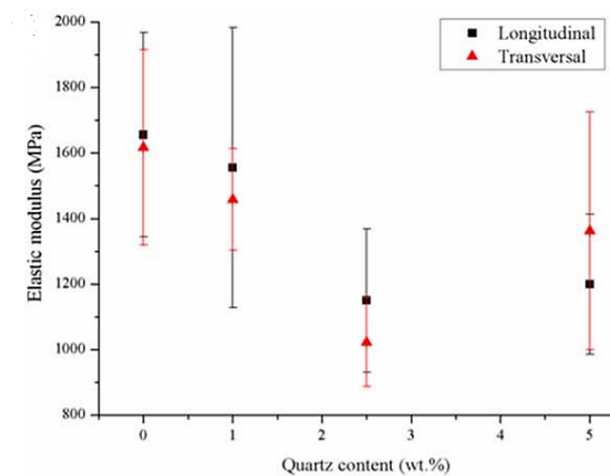


Figure 2.4: Tensile strength of PP-quartz composites films (Pérez et al., 2015)

Table 2.3 show that the increment of quartz loading level does not affect much for the thermal properties and degree of crystallinity. Quartz loading level 1wt% with longitudinal direction illustrated the maximum tensile strength among all. Tensile strength increased in 30% for 1wt% quartz content compare with pure polypropylene.



## 2.4 HDPE composites

Huang, et al. (2013) use the glass fiber or talc as filler and mixed with HDPE with different loading level to find out the performance for the composites material. The result show that increase the loading level for glass fiber can increase the tensile strength and flexural strength, especially at 30% of glass fiber loading. Next, the use of talc combined with glass fiber as filler can improve the recyclability and decrease the composite cost. In fact with increment of loading level, the linear coefficient thermal expansion (LCCTE) values for the composites material reduced.

Besides of glass fiber, HDPE composites could also be formed with recycled fillers. Waste printed circuit boards powders (WPCBP) had been accumulated by millions of tons and may cause pollution to the environment. The recycled WPCBP could become filler for HDPE. The result show that incorporation of WPCBP into the HDPE-wood composites can increase the strength, water absorption rate, viscosity and decrease the oxidation induction time (Tian, et al., 2017).

Scientists also tried to use recycle material like recycled HDPE fiber as raw material to create a new green composite material. Pešić, et al. (2016) mixed the concrete with the recycle HDPE fiber. Their results are encouraging, although the elastic modulus of concrete were unaffected, but the tensile strength and flexural modulus were marginally increased between 3% and 14%.

Wood filler or sawdust can be improve the strength for HDPE-wood composite, however the incompatibility make the degradation of strength after certain loading. Hence, Tazi et al. (2015) use coupling agent, Maleic Anhydride grafted Polyethylene (MAPE) to the HDPE-wood composite to maximize tensile strength for the composite. The results show that tensile strength is at the maximum with 40wt% loading of wood flour into

HDPE matrix with 3% of coupling agent. 54% of tensile strength increment in this filler loading when compared with pure HDPE.

Organic material also can act as a filler for polymer composites. Pineapple fibre are mixed with HDPE to make HDPE-pineapple fibre composites. However, addition of pineapple fibre does not reinforce the tensile strength for the composites materials. The study show that the tensile strength will be drop linearly with the increase of filler loading (Bahra, Gupta and Aggarwal, 2017). The low tensile strength is caused by the delamination and breakage of the fiber. The tensile strength could be improved with pre-treatment but the extra cost for pre-treatment need to be take into the consideration.

Badache, et al. (2018) had used 15wt% to 60wt% loading of recycle HDPE in mortar and immerse the composites in lime water for 28 and 90 days before conducting compressive strength test. The results are shown in Figure 2.5.

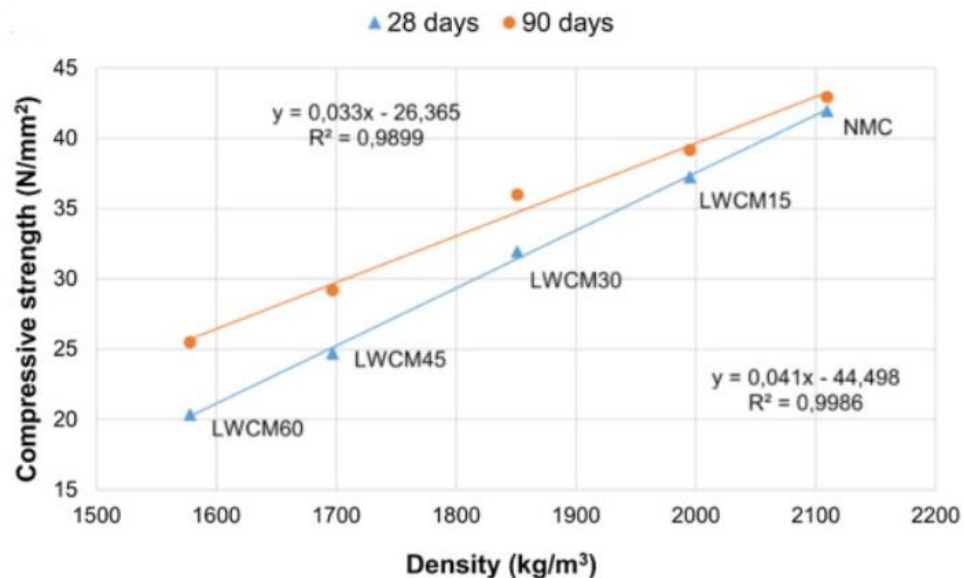


Figure 2.5: Relationship between compressive strength and density of mortar in the dry state (Badache et al., 2018).

The result shows that by increasing the loading of HDPE, the compressive strength and density will decrease. Immersing the composite in the lime water for longer duration results in the increase of compressive strength but no effect on the density.

Kelnar et al. (2018) prepared composite of HPDE/Nylon with the graphite nanoplatelets (GNP). Young's Modulus, maximum stress and elongation at break for the composites were increased up to 40% when compare with neat HDPE or neat Nylon.

Thermal properties for HDPE-jute composites and treated composite with MAPE were studied by Mohanty, Verma and Nayak (2006). TGA curve for composites is shown in Figure 2.6, from the curve, the main decomposition temperature was around 520°C. At this point, the residue drop dramatically and left less than 5%. Composites treated with MAPE (d) show better thermal stability them untreated HDPE-jute composite.

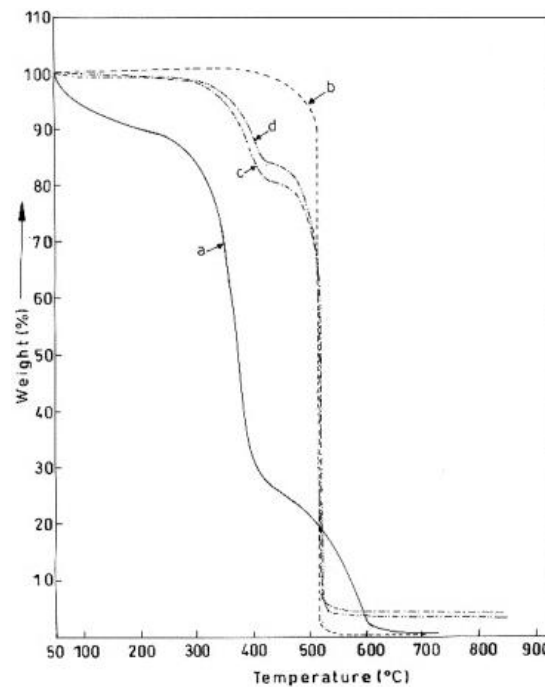


Figure 2.6: TGA curve for a) jute fiber, (b) virgin HDPE, (c) untreated composite, and (d) treated composite (Mohanty, Verma and Nayak, 2006)

Myristic acid (MA)-HDPE composites with nano-graphite and nano- $\text{Al}_2\text{O}_3$  were prepared for and studied the thermal properties (Tang et al., 2016). The MA loading was maximize at 70wt% of composite, and the nano-addictive does not affected the  $T_m$  which are constant at around  $50^\circ\text{C}$  for all sample. Furthermore, the thermal conductivity for the nano-graphite treated composites were better than nano- $\text{Al}_2\text{O}_3$  with same 12% mass ratio. The thermal conductivity is  $0.3972\text{ W/mK}$  for nano- $\text{Al}_2\text{O}_3$  and  $0.4503\text{ W/mK}$  for nano-graphite.

Next, the mica and wollastonite filler with HDPE composites were studied by Lapčik et al. (2018). Filler loading for both filler were set at 5wt%, 10wt% and 15wt% respectively. Figure 2.7 show the thermal analysis for the both HDPE composites.

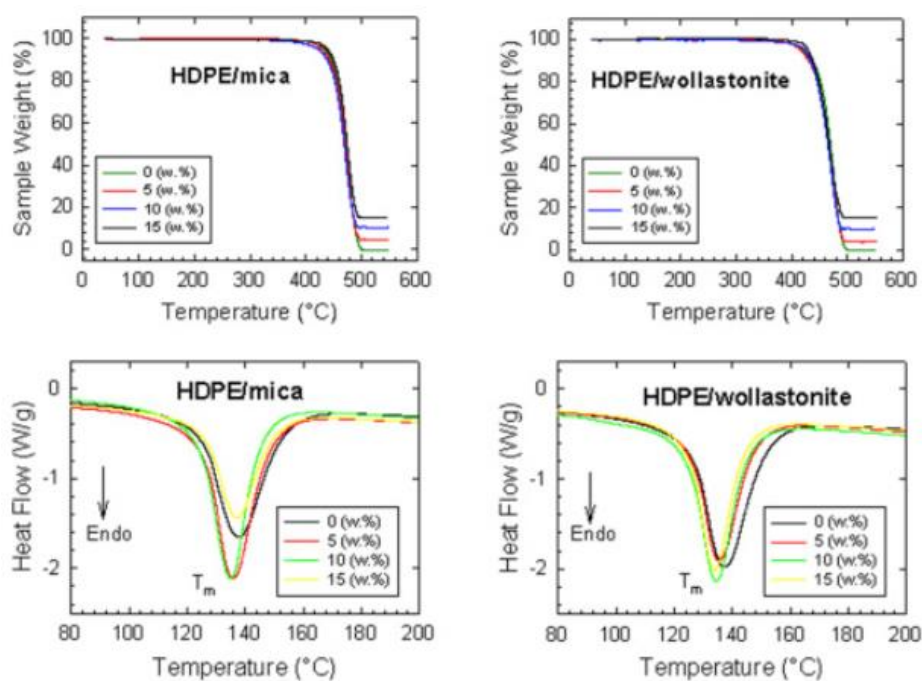


Figure 2.7: Thermal analysis results of the studied HDPE-mica and HDPE-wollastonite composites (Lapčik et al., 2018)

The analysis curves in Figure 2.7 show the crystallinity of HDPE-mica composites with 20wt% loading increase about 20% compared with neat HDPE, but decrease in 6% of crystallinity for HDPE-wollastonite composites with same filler loading amount. For both type of HDPE composites, they have similar thermal degradation rate which were about 460 °C, and the 15wt% filler loading show the best thermal stability among all filler loading.

HDPE-organically modified montmorillonite (OMMT) composites can be form high strength fiber. The research show that the highest modulus for the HDPE-OMMT composite can hit up to 38 GPa and 1.7 GPa of tensile strength with 6 wt% of OMMT loadings. Table 2.4 show the thermal properties and crystallinity for HDPE-OMMT composites with 6% OMMT loading and neat HDPE (Chantrasakul and Amornsakchai, 2007).

**Table 2.4: Thermal properties for HDPE and HDPE with 6 wt% OMMT in as-spun and drawn fibers (Chantrasakul and Amornsakchai, 2007)**

Samples	Peak melting temp. (°C)		Normalized crystallinity (%)	
	HDPE	HDPE + 6% OMMT	HDPE	HDPE + 6% OMMT
As-spun	128.6	128.0	46.2	47.8
10x	129.8	129.8	53.6	50.2
15x	130.8	130.7	53.6	58.7
20x	132.4	131.3	53.2	60.8
25x	132.9	132.5	58.1	62.2
30x	-	132.4	-	60.8
35x	-	132.6	-	81.9

The results indicate there are no much different change in the peak melting temperature, which maintain around 130°C. Although increase the drawn fiber increase the crisyallinity for HDPE and HDPE-sand composite, but the different among them with same drawn ratio is no much diffferent.

## **2.5 Building Materials**

There are various type of materials that are suitable for use in construction. Traditional natural building materials include of wood, mud and clay, stone and so forth. Next, human start to invent hand-made or synthesis material for construction purpose like reinforcement concrete and metal to increase the durability and strength of the buildings.

Concrete is the most common building materials nowadays. The concrete is weak in tension, and shrinkage of concrete causes crack development and strength loss (UKEssays, 2013). Cracking surface of the reinforcement will cause water or moisture penetrate into the core and make the cracking severe and corrode the reinforcement steel bar. Curing time for concrete is long, it at least take 7 days to 28 days for concrete to cure and reach the required durability and strength (Kewalramani, 2014).

Hence, the idea of using polymer or recycle polymer and other sustainable material that suitable to employ in the building material had become popular. Kulshreshtha et al., 2017 proposed the mixing of water with corn starch and sand to become a hardened concrete. Starch was used as the building material because starch is a natural polymer and renewable. The result show that, the concrete strength could be increased up to 26 MPa. However, the exposure to wet condition and moisture have limited the life cycle of concrete due to degradation.

Wood sawdust, plastic waste and polystyrene were mix together to become composite material and used in the building industry. By recycling the plastic waste, it can help to clean up the environment. Table 2.5 shown only in Benin, a country in Africa, there are total of 8500 tons of plastic waste for landfill. Granular composition of the wood particles will affect the physical properties of the composites materials like density, modulus of elasticity, modulus of rupture, water absorption and thickness swelling. The results was tabulated in Table 2.6, wood plastic composites with 4 granular compositions size of mixture gross increased the modulus of elasticity up to 100% compared with other compositions sample. However the composites materials not suitable to produce building block but it can become the material for furniture (Chanhoun et al., 2018).

**Table 2.5: Quantity of plastic waste in the cities of Benin (Chanhoun et al., 2018)**

N°	Plastic type	Tons of plastic waste in the cities of Benin					Percentage
		Cotonou	Porto- Novo	Parakou	Other cities	Total	
1	HDPE	2314.67	84.47	118.17	544.27	3061.58	36.30
2	LDPE	191.25	534.00	244.79	3440.85	4410.89	52.29
3	PP	32.09	28.16	-	181.42	241.67	2.87
4	PET	103.49	12.20	126.61	78.64	320.94	3.8
5	PVC	-	7.21	8.44	46.44	62.09	0.74
6	PS	-	18.93	16.88	121.98	157.79	1.87
7	PUR	81.87	12.01	8.44	77.44	179.72	2.13
8	Total	2723.37	696.98	523.34	4491.00	8434.69	100

**Table 2.6: Physical and mechanical properties of wood composites plastic and polystyrene (Chanhoun et al., 2018)**

Sample designation	Diameter of the particles (mm)	Compaction rate (%)	Absorption (%)	Density (g/cm <sup>3</sup> )	Thickness swelling (%)	MOE (MPa)	MOR (MPa)
P-WPsC-Cg1-D1.5	0.630 < d < 1.25	17	19.07	0.667	9.09	2830.678 ± 68.17 0	21.244 ± 0.76 6
P-WPsC-Cg2-D1.5	0.315 < d < 0.63 0	27	16.33	0.721	2.86	2325.752 ± 34.70 1	20.096 ± 0.67 0
P-WPsC-Cg3-D1.5	0.16 < d < 0.315	30	11.39	0.770	2.00	2057.821 ± 28.29 5	14.067 ± 0.67 0
P-WPsC-Cg4gross-D1.5	0.16 < d < 1.25	21	18.91	0.757	0	4604.893 ± 39.80 5	16.507 ± 1.05 2
P-WPsC-Cg4fine-D1.5	0.16 < d < 1.25	28	19.14	0.720	5.0	2147.222 ± 22.15 1	11.914 ± 0.95 7
P-WPC-Cg1-D3.0	0.630 < d < 1.25	-	16.02	0.981	0	694.883 ± 43.160	5.732 ± 0.695

Pešić et al. in 2016 use the recycle HDPE plastic fiber composites with the concrete for construction industry. HDPE fiber increase the post-cracking ductility and improved serviceability properties of the composites, reduce water permeability and shrinkage. The shrinkage crack of the concrete with different loading of fibers are shown in Figure 2.8.



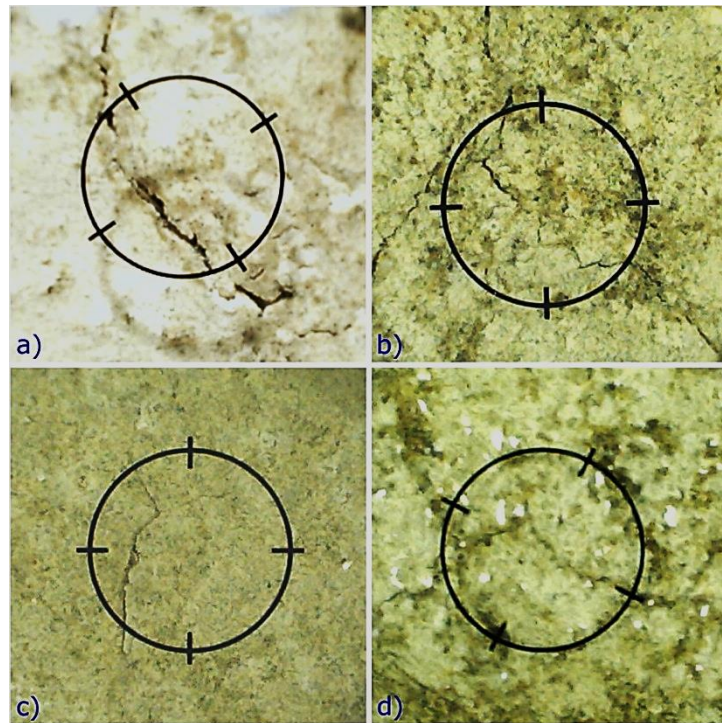


Figure 2.8: Plastic shrinkage cracks on the surfaces of: a) plain concrete, and b), c) and d) FRC with 0.40, 0.75% and 1.25% fibers, respectively with  $40\times$  magnification (Pešić et al., 2016)

The reinforced concrete with higher loading of fiber show the least crack. Addition of HDPE fiber to concrete can significantly reduce the water permeability up to 42%. Less water penetration to the concrete can improve the durability and strength. Hence the depletion of shrinkage crack is noticeable, more than 50% improvement by only 1.25% of fibres are added.

## 2.6 Filler

Filler is added into polymer in order to improve the physical and mechanical properties or to reduce the cost. There are variety of filler like organic, inorganic and natural filler. They also vary in shape and size; spheres, long or short fibres and irregular shape. Filler with

narrow particle-size distribution have worse packing in polymer matrix and increases the viscosity when compared with broad particle-size distribution. Hence, broad particle-size distribution is normally recommended (Tsou and Waddell, 2004).

Wang et al. in 2017 tested the electrospun nanofibers as the filler for polymer composites. Different size of nanofibres; long and short fibre were used. Over loading of long nanofibers, about 0.3wt% in the polymer nanocomposite (PNC) will cause the decrement of mechanical properties. For short fibre, the optimum loading usually is higher because it cause less agglomeration at same loading level as long fibre. Increment of loading level for short fibre can go up to 40wt% and still maintain the mechanical performance for the composite.

The most important factor that affect the mechanical properties of the composites is the strength of interaction between the polymer and filler particle and the structure of the filler surface (Feng, Venna and Hopkinson, 2016). The interaction between the polymer and filler particle could be changed from repulsive to attractive and can increase the polymer density and decrease the free volume fraction. Hence the polymer becomes stronger. Ferdous et al., 2016 research was on the resin to filler ratio affect to the physical properties on the composite railways sleepers. The results showed that the fillers loading from the range of 30% to 50% show the optimum performance in term of durability and cost effectiveness.

Organic filler always used to mix with concrete to improve the strength. Fly ash and bitumen emulsion were added into the cement to improve the composite's properties like compressive strength, density and water absorption (Bołtryk, Krupa and Pawluczuk, 2018). Echeverria et al. in 2017 prepared hybrid wood-polypropylene bio-composite with 60/40wt% loading, and particle size was 20 to 40 mesh respectively. Then, they added secondary bio-fillers to the composite at 10 and 20 wt% loading. As expected, the

performance of bio-composites in term of water absorption and thickness swell had been maintained below 28% and 0.6% respectively for composites. Physical and mechanical properties for the bio-composites are shown in Table 2.7. The performance in term of thickness swelling is remarkably below 21% of ISO requirement. Hence, the bio-composite is also suitable for high-moisture environment applications.

**Table 2.7: Summary of physical and mechanical properties of Hybrid Wood-Polypropylene Bio-composite (Echeverria et al. in 2017)**

Panel Type	Formula wt%	Mesh number	Density g/cm <sup>3</sup>	Mechanical			Moisture	
				MOR MPa	MOE GPa	Elongation %	WA %	TS %
Panel A	40/20/20/20	20	0.83	3.64	1.03	2.65	32.7	2.4
Panel B	40/40/10/10	20	0.81	6.75	0.83	2.62	36.8	0.6
Panel C	40/40/10/10 +MAPP	20	0.76	11.99	1.32	3.35	27.8	2.5
Panel D	40/40/10/10	40	0.85	11.13	1.04	3.88	30.9	4.6

## **CHAPTER 3**

### **METHODOLOGY**

#### **3.1 Materials**

HDPE-sand composite was prepared to be used in construction industry in future. The HDPE was supplied by Azlon Plastics United Kingdom with density of  $950 \text{ kg/m}^3$  and  $7.17 \text{ g/10min}$  MFI value. And the sand was obtained from the construction area of Agacia Land, Kampar.

#### **3.2 Preparation of HDPE-Sand Composite**

Collected sand was pre-dried in oven for 24 hours at  $80^\circ\text{C}$  to remove the moisture absorbed on the sand. Next, the dried sand was sieved using  $150 \mu\text{m}$  mesh. Sand that pass through the  $150 \mu\text{m}$  mesh was collected and used further. The composites were produced by melt mixing method in the Brabender® Plastograph® EC 815652 internal mixer. 50g of HDPE pellets were premixed well with sieved sand and loaded into the internal mixer with the operating temperature of  $180^\circ\text{C}$ . The rotor speed for the internal mixer was set at

60rpm. The mixing process was allowed to take place for 8 minutes until the HDPE pellets and sand were mixed homogenously. Next, the torque and temperature profile for the mixing process was recorded. The loading of sand were fixed at 20, 40 and 60 wt%.

HDPE-sand composite samples for testing were fabricated by using hydraulic hot and cold press model GT-7014-A30C. The moulding temperature was set up at 180°C to press the HDPE-sand composite materials. Preheating was done for 10 minutes, followed by 5 minutes pressing and 2 minutes for cooling. The formulation for compounding is as listed in Table 3.1.

**Table 3.1: Weight of HDPE and Sand for Compounding**

Weight Percentage of Sand (wt%)	Weight of HDPE (g)	Weight of Sand (g)	Ratio HDPE: sand
0	50	0	1:0
20	40	10	4:1
40	30	20	3:2
60	20	30	2:3

### 3.3 Characterization

#### 3.3.1 Particle Size Analysis (PSA)

Malvern Mastersizer 2000 PSA machine was used to analyze the particle size for sand. The analysis was to make sure the particle size of sand was smaller than 150 $\mu$ m. The refractive index used for the test is 1.4585.

### **3.3.2 Morphology Study**

Morphology for sand sample and the HDPE-sand composite under the magnification of x10,000 was observed using the Field Emission Scanning Electron Microscopy (FESEM) model JEOL JSM 6701F at the accelerating voltage of 2kV. Before proceed to the scanning process, the samples were placed on a disc and held by double-sided carbon tape. Then, the samples were coated with platinum particles to avoid charging effect.

### **3.3.3 Fourier Transform Infrared Spectroscopy (FTIR)**

FTIR test was carried out using PerkinElmer Spectrum ex1 to identify the chemical bonds and functional groups in the sand and HDPE-sand composites. Sand sample which was in powder form was measured using Potassium bromide (KBr) method while the HDPE-sand composites was analyzed using Attenuated Total Reflection (ATR) method. FTIR analysis was carried out at wavelength between 400 to 4000 $\text{cm}^{-1}$  with step scan 4 and resolution of 4 $\text{cm}^{-1}$  to measure the absorption band of the substances. The background of spectrum was captured before the samples were scanned to obtain the infrared intensity without sample.

### 3.3.4 Thermal Decomposition Study

Thermal Gravimetric Analysis (TGA) was done using Mettler Toledo TGA SDTA851 e machine on the composite. The analysis was conducted from 25 to 800°C with the increment of heating rate at 10°C/min in nitrogen atmosphere. The normal curve and derivative curve for the TGA result were obtained.

### 3.3.5 Thermal Properties Analysis

Differential Scanning Calorimetry (DSC) for the research was done using Mettler Toledo DSC 1/500 machine. Melting behavior, crystallization and crystallinity of the HDPE-sand composites was characterized. The analysis was carried out by heating from room temperature to 250°C at heating rate of 10°C/min in air atmosphere for cooling and heating.

The crystallinity was calculated from Equation 3.2:

$$X^m_c = \frac{(\Delta H_m - \Delta H_c)}{\Delta H_m^\circ} \times 100\% \quad (3.2)$$

Where

$X^m_c$  = Degree of crystallinity (%)

$\Delta H_m$  = Heat of melting (J/g)

$\Delta H_c$  = Cold crystallization (J/g)

$\Delta H_m^\circ$  = heat of melting 100% crystalline HDPE, 231.86 J/g

### **3.3.6 Melt Flow Index (MFI)**

MFI was proceeded to measure the ease of flow for HDPE-sand composites in molten state. The machine used for MFI was Tinius Olsen Extrusion Plastometer model MP600 and Procedure A of ASTM D1238 was employed for testing purpose. The total mass of HDPE-sand composites that were extruded from the die was weighted and calculated in g/10min.

### **3.3.7 Energy-dispersive X-ray spectroscopy (EDX)**

The elemental analysis or chemical characterization of the sand filler was being confirmed by the Energy-dispersive X-ray spectroscopy (EDX) using JEOL JSM 6701F at the accelerating voltage 2kV. Three runs of scanning for the sand filler were done.

## **3.4 Performance Test**

### **3.4.1 Tensile Test**

Tensile test was carried out in accordance to ASTM D638 standard under ambient condition. Tensile test equipment Tinius Olsen H10KS-0748 was used for this purpose. Elastic modulus, elongation at break and ultimate tensile strength of the composites were obtained. Test sample was pre-cut by using dumbbell press cutter. The load cell for the machine was set at 500N with crosshead speed of 50mm/min. Length, thickness and width for the sample gage were measured. Seven samples were used in each formulation set to get a valid result. FESEM images was taken on the tensile fracture surface.



### 3.5 Flow Chart

Flow of the research work is summarized in Figure 3.1.

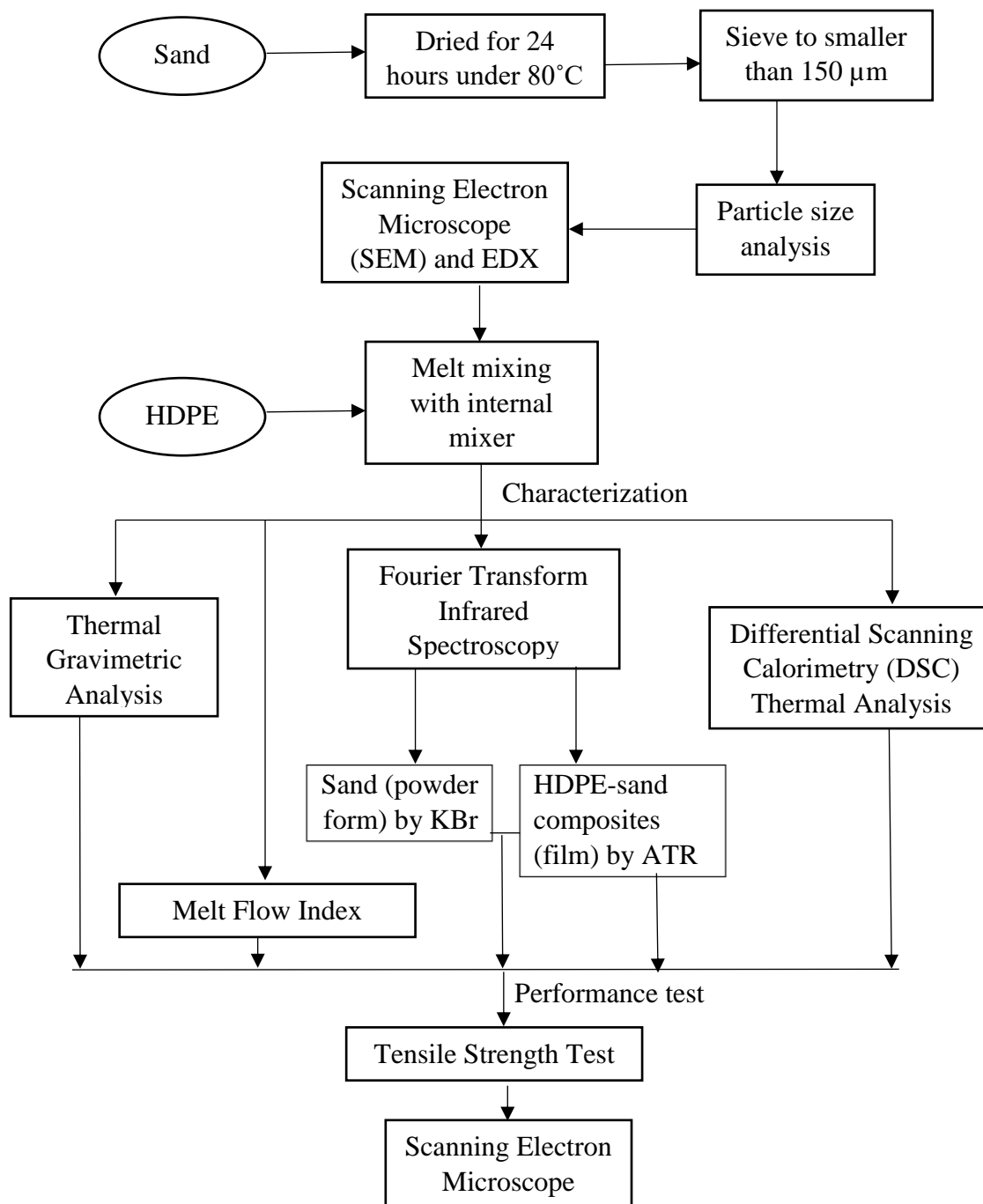


Figure 3.1: Flow chart of methodology

## **CHAPTER 4**

### **RESULTS AND DISCUSSIONS**

#### **4.1 Characterization of Sand Filler**

Physical, chemical and morphology of the sand filler was characterized using FTIR, SEM-EDX and FESEM images.

##### **4.1.1 Fourier Transform Infrared Spectroscopy (FTIR)**

FTIR was carried out to identify the functional groups of sand. Figure 4.1 shows the IR spectrum of sand and Table 4.1 summarizes the absorption frequency regions for the relevant functional groups in sand.

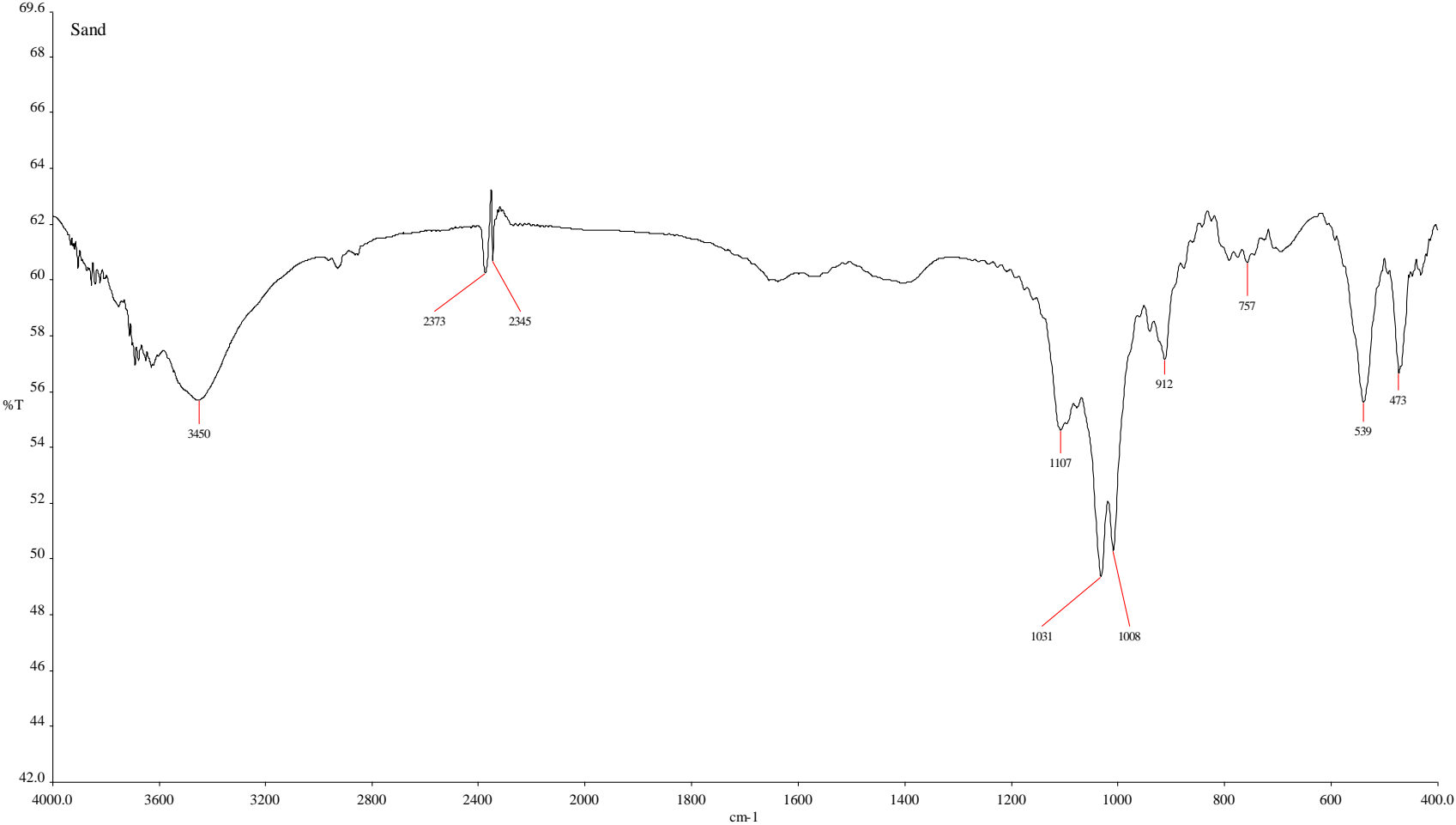


Figure 4.1: FTIR spectra of sand

**Table 4.1: Functional Groups and Absorption Frequency Regions**

Absorption Frequency (cm <sup>-1</sup> )	Functional Group
Sand	
3450	O-H Stretching
1107	C-O Stretching
1031	Si-O Stretching
1008	C-O Stretching
912	Illite Group
757	Symmetric Si-O Stretching
473	Asymmetrical Si-O Bending

1031 cm<sup>-1</sup>, 757 cm<sup>-1</sup> and 473 cm<sup>-1</sup> peaks are the common quartz IR peaks that can be found in the spectra (Müller et al., 2011). These peaks represent Si-O stretching, symmetric Si-O stretching and asymmetrical Si-O bending. Next, O-H group also form intense peak at 3450 cm<sup>-1</sup>. This peak is observed due to surface bound water or moisture on the sand (Ellerbrock and Gerke, 2004). 1107 cm<sup>-1</sup> and 1008 cm<sup>-1</sup> peaks show the functional group of C-O stretching in the spectra. These peaks show phosphate or nitrate impurities in sample that caused by fertilizer-originating phosphate or nitrate (Bernier et al., 2013). Another notable peak from the spectra is 912 cm<sup>-1</sup> which represent illite group. Illite is non-expanding micaceous mineral that form under weathering and hydrothermal environments which is commonly found in soil and sedimentary rock. (Chandrasekaran et al., 2015).

### 4.1.2 Energy-dispersive X-ray spectroscopy (EDX)

Elemental analysis or chemical characterization of the sand filler was being confirmed by the Energy-dispersive X-ray spectroscopy (EDX). Three runs of scanning were done and the results were summarized in Table 4.2.

**Table 4.2: Summary of EDX spectrum in wt%**

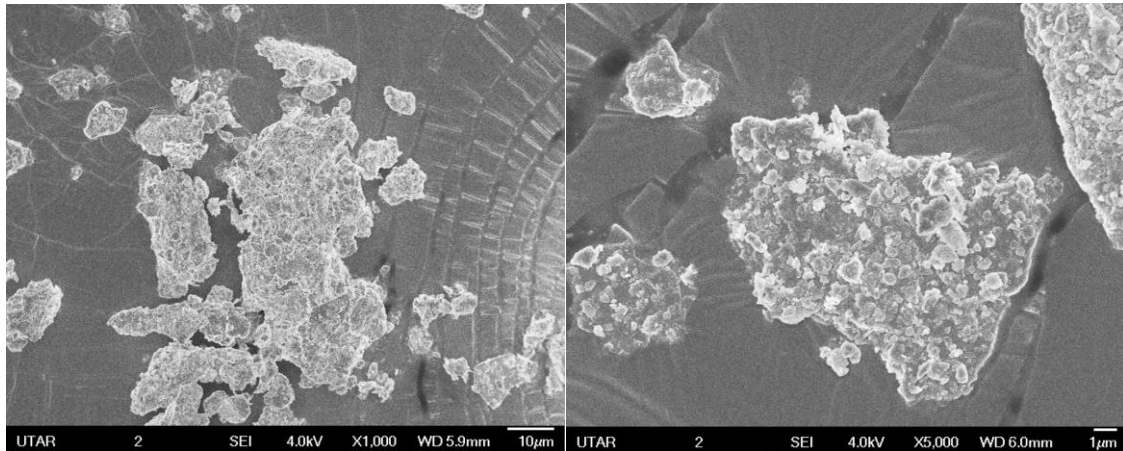
<b>Spectrum</b>	<b>C</b>	<b>O</b>	<b>Al</b>	<b>Si</b>	<b>K</b>	<b>Ca</b>	<b>Cu</b>	<b>Mo</b>
<b>Spectrum 1</b>	19.16	58.08	1.99	20.41	0.09	-	0.26	-
<b>Spectrum 2</b>	22.74	53.45	2.28	21.53	-	-	-	-
<b>Spectrum 3</b>	28.85	53.01	2.36	14.95	0.11	0.13	0.26	0.34

Table 4.2 shows that sand has high weight percent of silicon (Si) and oxygen (O) and carbon (C) element. Other elements from EDX spectrum are commonly found in fillers from mineral source. Sand filler sample is mainly made up by silicon dioxide ( $\text{SiO}_2$ ) and carbon. The high level of C in the spectrum is because of carbonate content carbonate normally origin from continental shelf sea (Fioravante, Giretti and Jamiolkowski, 2013). The EDX spectrum summary for the test is shown in APPENDIX A.

### 4.1.3 Morphology Study

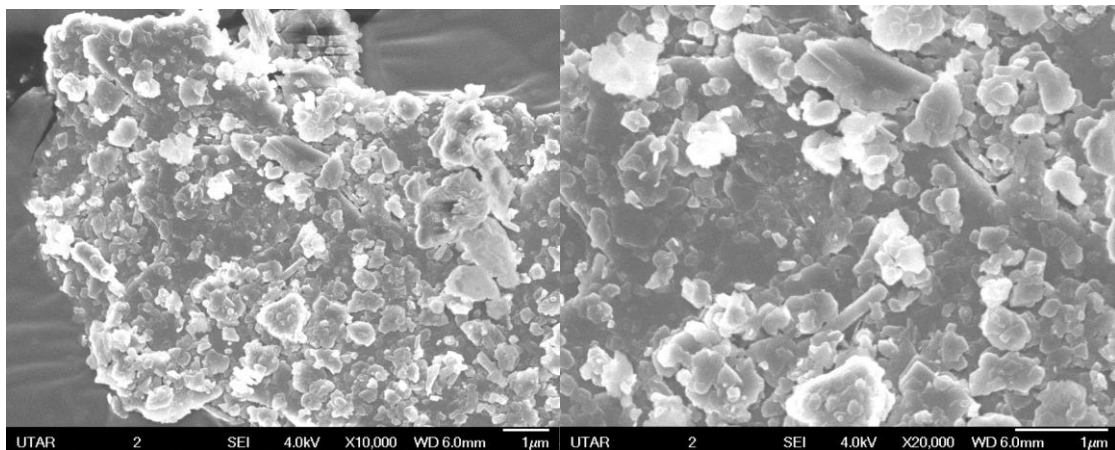
The morphology of sand filler was examined using FESEM. Flake like shapes of sand fillers were observed in Figure 4.2. This was similar with the morphology reported by

Manoharan et al. (2018). Higher content of  $\text{SiO}_2$  will result to more flakes shape morphology due to elimination of voids between the particles.



(a)

(b)



(c)

(d)

Figure 4.2: SEM images of sand at (a) 1000x, (b) 5000x, (c) 10000x and (d) 20000x magnification

#### 4.1.4 Particle Size Analysis

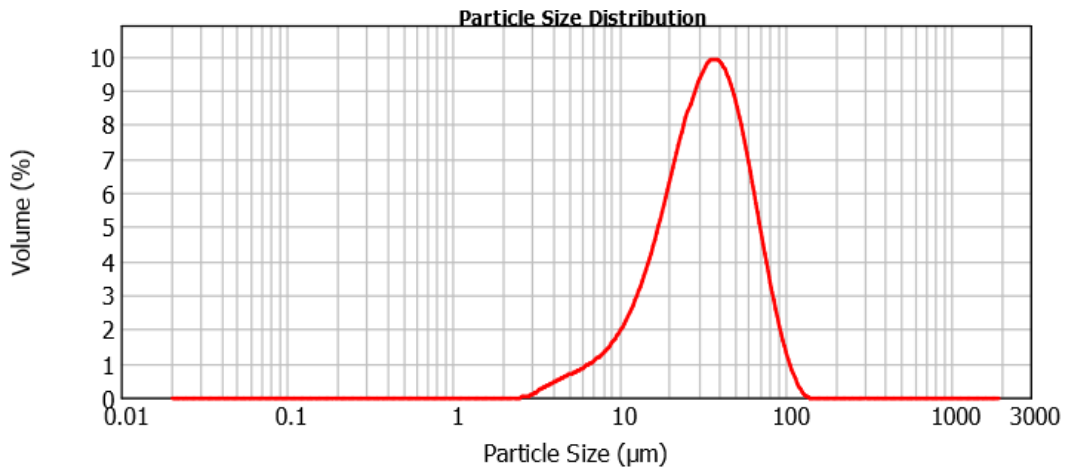


Figure 4.3: Particle size distribution for sand

Before the melt blending process to mix the sand with HDPE, the sand was sent to sieve using mesh of 150  $\mu\text{m}$  to ensure the internal mixing is easier and less wear and tear to the machine. Figure 4.3 shows that the mean of particle size distribution is around 33  $\mu\text{m}$ , while the overall particle size was ranging from 120 to 200  $\mu\text{m}$  which is in the acceptable range compared to previous works. In work by Subaşı, Öztürk and Emiroğlu (2017), waste ceramic powder was used as filler with self-consolidating concrete to improve the mechanical performance of composite. Ceramic powder with particle size of 125  $\mu\text{m}$  has induced good fresh state properties, strength and durability in the composites. In another research, Roman and García-Morales (2018) had used mineral fillers with particle size from 10-50  $\mu\text{m}$  together with polyethylene-bitumen mastics. In addition, the specific surface area for sand filler sample in this study is 0.253  $\text{m}^2/\text{g}$  based on particle size analysis report which shown in APPENDIX E.

## 4.2 Processing Characteristics of HDPE-Sand Composite

Figure 4.4 shows the temperature profile for pure HDPE and its composites with time from internal mixer. For neat HDPE, the processing time is 8 minutes but the composites are processed for 10 minutes to provide better mixing.

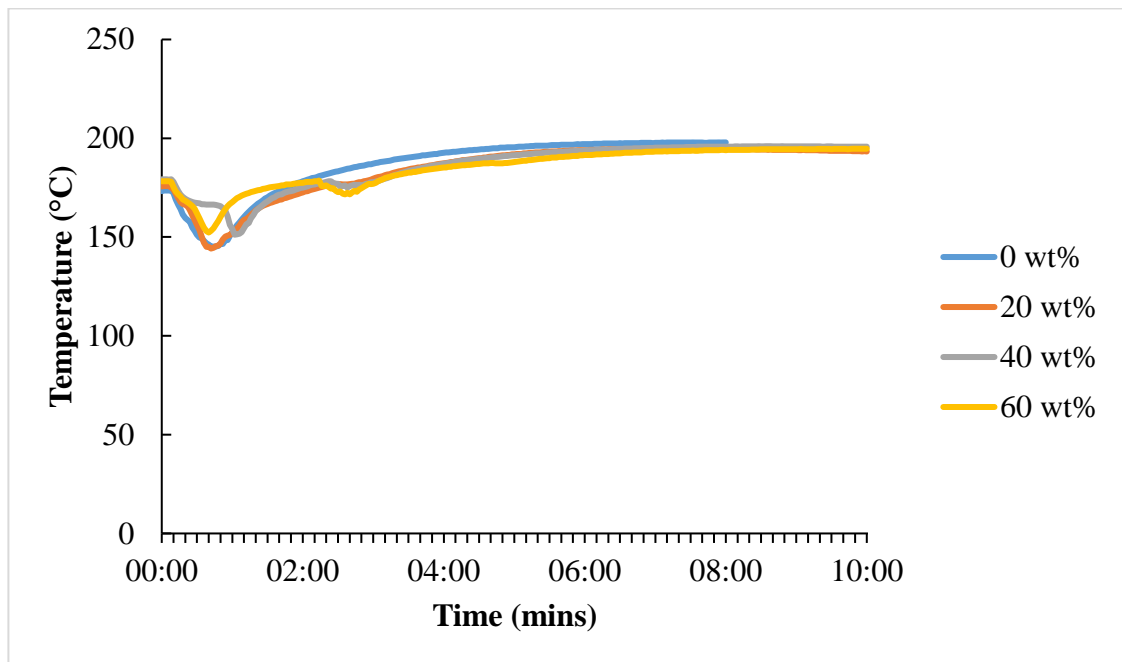


Figure 4.4: Temperature profile for neat HDPE and HDPE-sand composites

From Figure 4.4, the temperature profile demonstrate that temperature required for neat HDPE reach stability in term of processing torque is slightly higher than composites. Energy absorbed by HDPE with 60wt% sand filler is lower than neat HDPE due to reduction in melting temperature ( $T_m$ ) with increasing of sand loading as shown by Differential Scanning Calorimetric results in Section 4.3.2. According to literature thermal conductivity of sand in dry condition is 2.05 W/m/K (Hamdhan and Clarke, 2010) while thermal conductivity of HDPE is approximately around 0.49 W/m/K (Abee et al., 2014).



High thermal conductivity of sand will lead to better absorption of heat energy at the processing time provided thus the processing temperature observed for composites are lower than the processing temperature for neat HDPE.

Figure 4.5 shows the stabilization torque for all the composites are lower compared to neat HDPE, with the largest decrement in stabilization torque experienced by HDPE filled with 20 wt% sand filler. It has 27% stabilization torque lower than neat HDPE and this is due to good dispersion of filler in the composites. The well dispersed filler can lead to better shearing during processing, generate heat, reduce viscosity of the melt, reduce resistance to rotor rotation and enhance process ability. In general, stabilization torque can be used as a direct measurement for the viscosity of HDPE melt mixture in dynamic conditions in processing equipment (Ling, Ismail and Bakar, 2016).

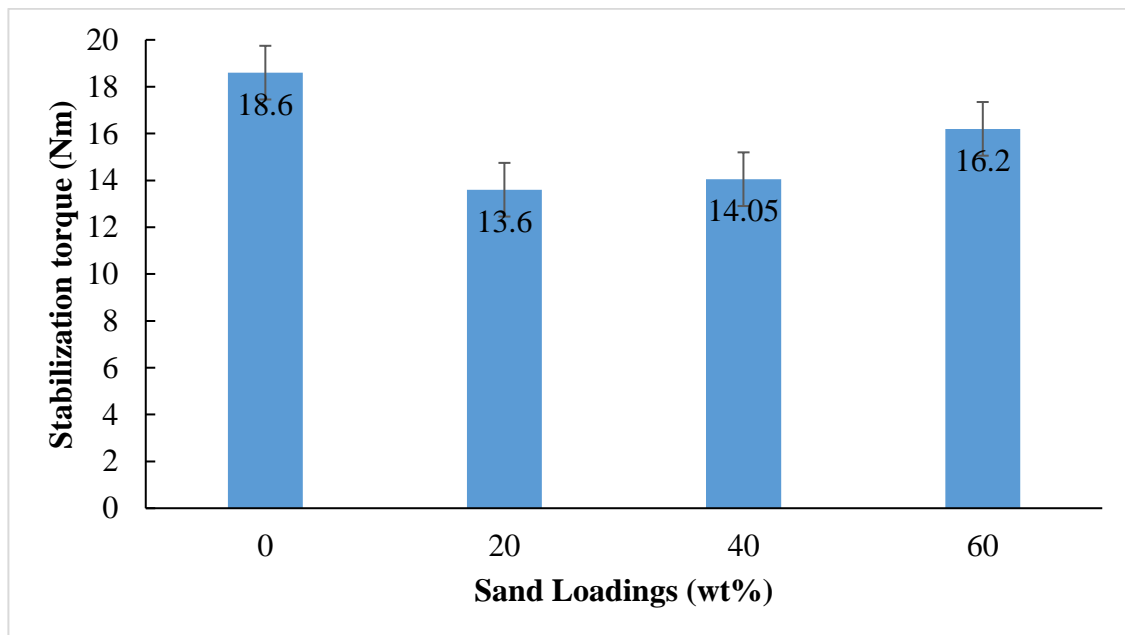


Figure 4.5: Stabilization torque for neat HDPE and HDPE-sand composites

### 4.3 Characterization of HDPE-Sand Composites

#### 4.3.1 Fourier Transform Infrared Spectroscopy (FTIR)

FTIR was carried out as a qualitative measurement on the functional groups of neat HDPE and HDPE-sand composites. Base on the spectra for HDPE, alkanes and alkenes functional groups have been observed (Kumar and Singh, 2011). All the frequencies and functional group were tabulated in Table 4.3.

**Table 4.3: Functional Groups of HDPE to Peaks in IR Spectra**

Frequency (cm <sup>-1</sup> )	Functional Group
2947	Alkane C-H stretch
1463	Alkane CH <sub>2</sub> bend
1367	Alkane CH <sub>3</sub> bend
1305	Alkenes C-H in-plane bend
966	Alkenes C-H bend (disubstituted - E)
888	Alkenes C-H bend (disubstituted - 1,1)
721	Alkane CH <sub>2</sub> bend (4 or more)

Figure 4.6 shows that when increasing the filler loadings, peak of alkenes and alkanes functional groups in HDPE composites become harder to observe. At the filler loading of 60wt%, IR spectra curve is almost same with the sand's spectra. However indication of formation of any chemical bonds or interaction between HDPE and sand was not observed. Thus in this work we proposed physical adsorption and interlocking of polymeric chain on the surface of sand filler rather than chemical interaction. This is mainly due to the hydrophobic nature of HDPE polymer matrix. APPENDIX B shows the IR spectra for each samples.

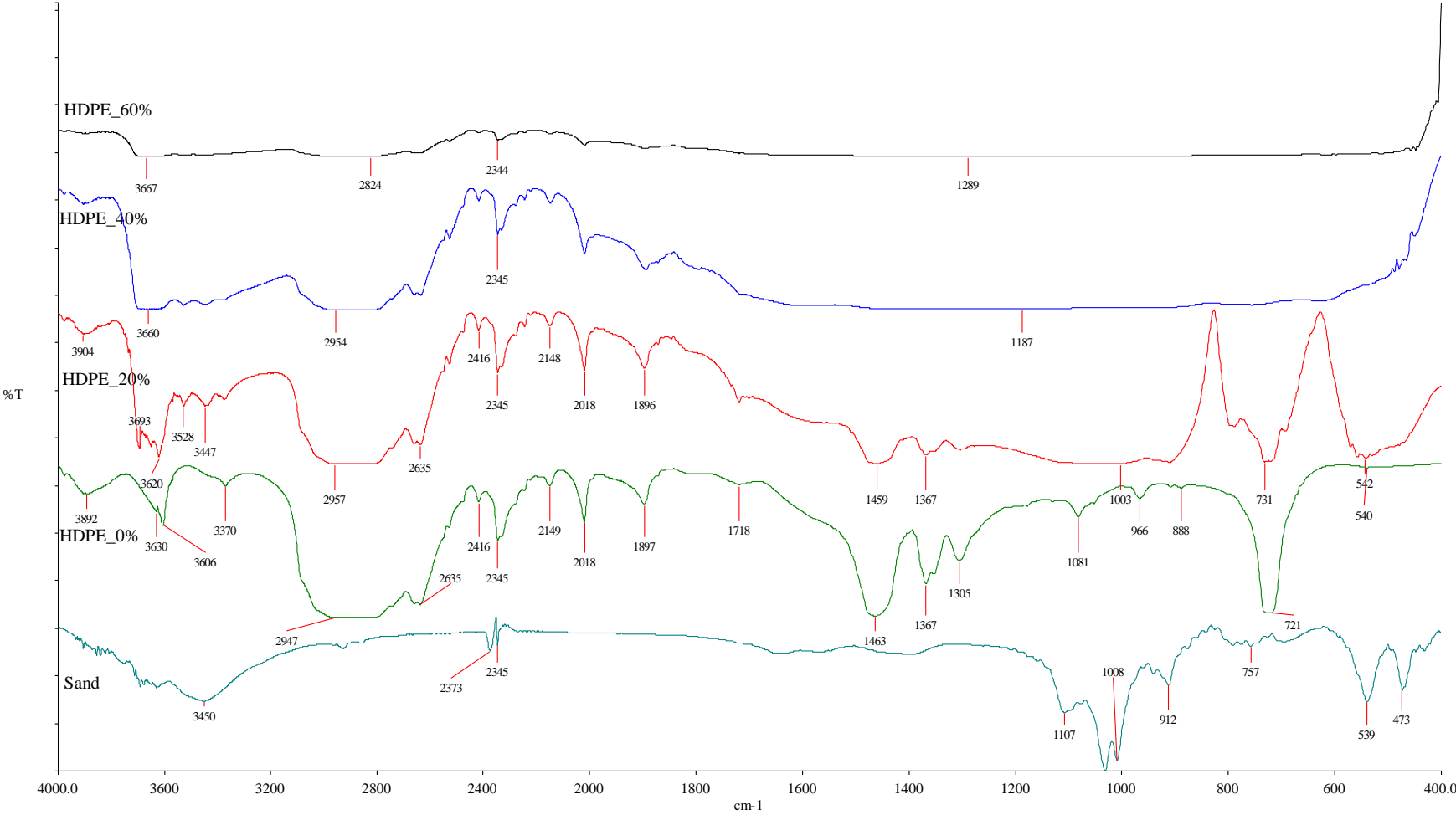


Figure 4.6: FTIR spectra for HDPE-sand composites

### 4.3.2 Thermal Properties of the HDPE-sand composites

DSC analysis can record the transitions or phase change of material with temperature. Melting temperature ( $T_m$ ) and crystallization temperature ( $T_c$ ) of neat HDPE were determined through the curve.  $T_m$  of neat HDPE is 135°C and  $T_c$  is 117°C. From Figure 4.7, the  $T_c$  for composites with all filler loadings are almost similar which indicates that the cooling temperature for the composites during moulding could be set as the same as pure HDPE.  $T_m$  slightly decrease with the increment of filler loadings which implies that the composites could be melted at lower temperature compared to HDPE during processing. All the data are shown in the APPENDIX C.

From Table 4.4, the most significant difference between all samples are the degree of crystallinity ( $X_c^m$ ).  $X_c^m$  for 20 wt% sand loaded composite is higher than neat HDPE. High degree of crystallinity could be attributed by good dispersion of filler. Well dispersed filler cause better nucleation for the polymer. Previous research by Lapčák et al. (2018) using mica as filler for HDPE showed increment in crystallinity by 20%. Similar finding was also reported by Sarasini et al. (2018) in HDPE filled with hemp fibre, where the crystallinity increases 15% compared to pure HDPE. However the crystallinity decrease as the filler loading increases more than 20 wt%. Degree of crystallinity for composites with 60wt% sand loading had dropped to 2.14%. This might be due to agglomeration of filler which cause disturbance in the growth of crystal groups (Shao et al., 2018). Agglomeration at loading more than 20 wt% sand were also evidenced from the torque reading in Figure 4.5. Lowest torque was achieved at 20 wt% loading while as the loading increases, the torque value increases which is an indication to the increment of resistance to the rotor rotation due to agglomeration.

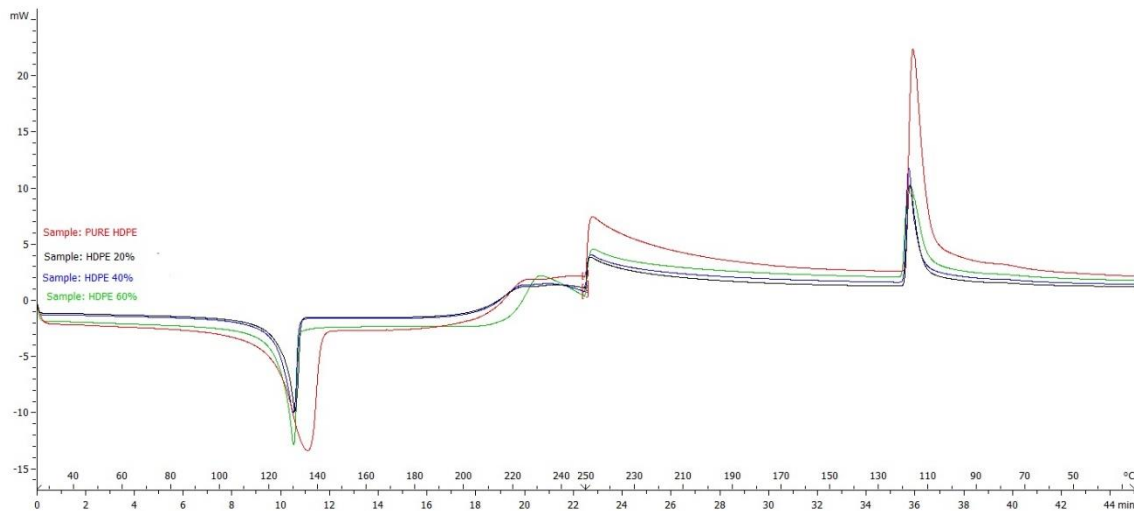


Figure 4.7: DSC Curves for HDPE-sand composites with different loading

**Table 4.4: DSC results of pure HDPE and composites**

Sand Loadings (wt%)	$T_m$ (°C)	$\Delta H_m$ (J/g)	$X_c^m$	$T_c$ (°C)
0	135.4	193.65	5.76	116.8
20	130.4	151.48	9.51	117.4
40	129.9	107.22	4.55	118.0
60	129.8	75.23	2.14	117.4

Where,

$T_m$  = Melting temperature

$\Delta H_m$  = Melting heat

$X_c^m$  = Degree of crystallinity

$T_c$  = Crystallization temperature

### 4.3.3 Melt Flow Index (MFI)

Melt flow ability of neat HDPE and composites were obtained by studying the MFI values. The results were compiled in Table 4.5.

**Table 4.5: MFI Values of pure HDPE and composites**

Sand Loadings (wt%)	MFI(g/10min)
0	7.17
20	15.78
40	5.06
60	1.28

HDPE-sand composites with 20wt% sand loading endows the best flow ability among all. This is caused by the well dispersion of sand filler in the composite matrix. In addition, better flow ability mean better process ability because of the ease of flow. The flow ability of composites with 40wt% and 60wt% are lower than neat HDPE. Agglomeration of large amount of filler will produce large energetic barrier for the movement of polymer chains and increase the activation energy for polymer to flow (Barus et al., 2010).

In general the decrement in stabilization torque is expected to yield higher MFI value. However the MFI value for composite filled with 40 and 60 wt% filler is lower compared to neat HDPE even though the stabilization torque value is less. This is due to the nature of flow in both equipment. Shear in dynamic condition in internal mixer will provide extra heat energy for polymer to melt, but in MFI the heat is supplied only by the

barrel wall of MFI equipment. Polymer is a very bad thermal conductor, thus it takes more time to melt and flow in MFI.

#### **4.3.4 Thermal Decomposition Study**

Thermal decomposition for neat HDPE and HDPE-sand composites were tested by using TGA under nitrogen atmosphere at a heating temperature from room to 800°C. From Figure 4.8, it could be observed that neat HDPE and all its composites showed one step decomposition where the mass-loss centred at temperature around 410- 510 °C. Hence, addition of sand does not alter the decomposition pathway for the composites. According to Kumar and Singh (2018), 50 wt% thermal decomposition for neat HDPE was reported to happen around 460°C. Increment of sand loading level, increases the thermal decomposition temperature and also increases the char formation. The composites become more stable hence more resistance against fire. The data was summarized in Table 4.6 and the raw curves for all samples are shown in APPENDIX D.

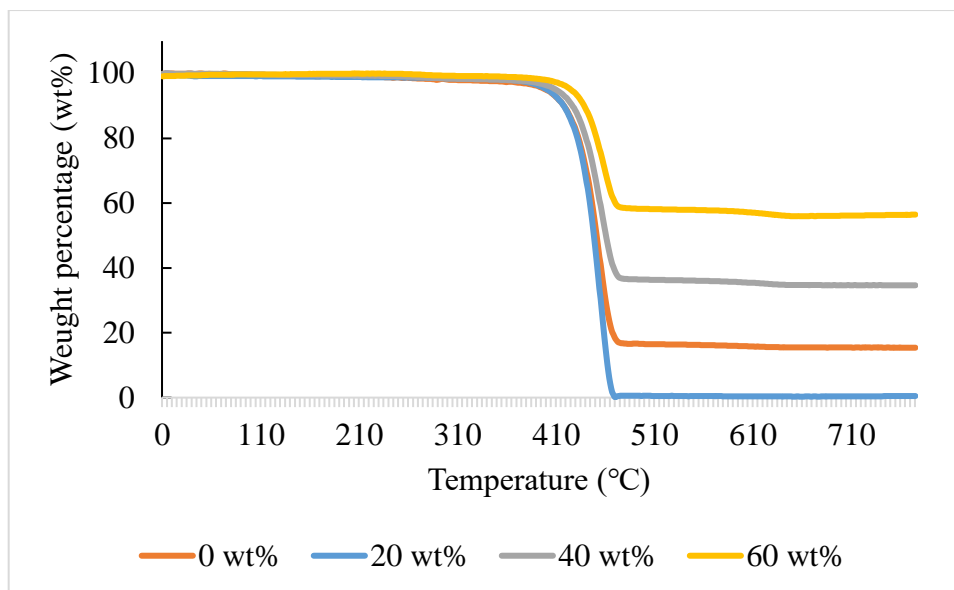


Figure 4.8: TGA curves for HDPE-sand composites

**Table 4.6: Temperature weight loss at 50wt% and 10wt%**

Sand loadings (wt%)	Temperature (°C) at 10wt%	Temperature (°C) at 50wt%
	weight loss	weight loss
0	441	472
20	441	475
40	450	484
60	462	NA because the weight loss is below 50%



## 4.4 Performance Tests of HDPE-Sand Composites

### 4.4.1 Tensile Test

The mechanical properties of HDPE-sand composites were studied by tensile test. Figure 4.9 to 4.11 provide the trend of Young's Modulus, tensile strength and elongation at break of neat HDPE and HDPE-sand composites. All the mechanical properties for the samples had been summarized in Table 4.7. Young's modulus indicate the stiffness of the material; higher Young's modulus mean more stiff samples. The tensile strength is the maximum stress that the sample can bear before break. Elongation at break also known as fracture strain, is the changed of length after the sample broke.

HDPE-sand composites at 40wt% sand loading has the highest Young's modulus, 1509 MPa hence it is the stiffest composites among all. To relate back to the problem statement, tensile result from this study is being compare with other research and tabulated in Table 4.8. Increment in Young's Modulus value of 62.25% recorded from this research work is comparable with others research in Table 4.8 for polymer composites developed for use as building materials. While the optimum tensile strength obtained, 26.50 MPa at 40 wt% sand filler loading is far more higher than the tensile strength required for mud bricks (1.9 MPa) and clay-fired brick (14 MPa) (McIntosh, 2014).

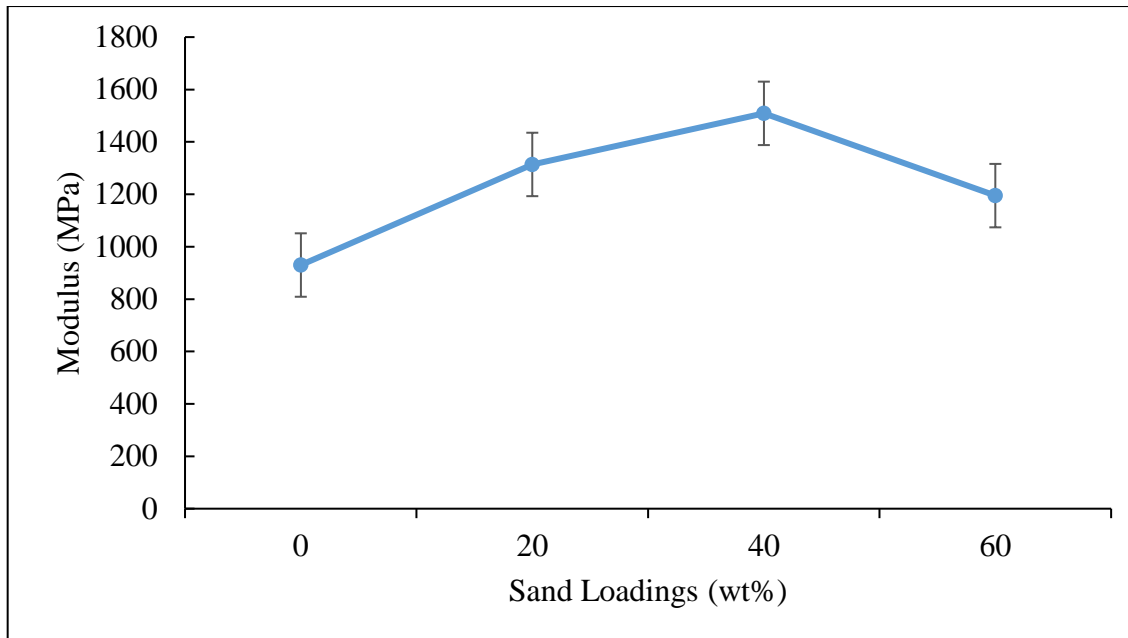


Figure 4.9: Young's Modulus of HDPE-sand composites

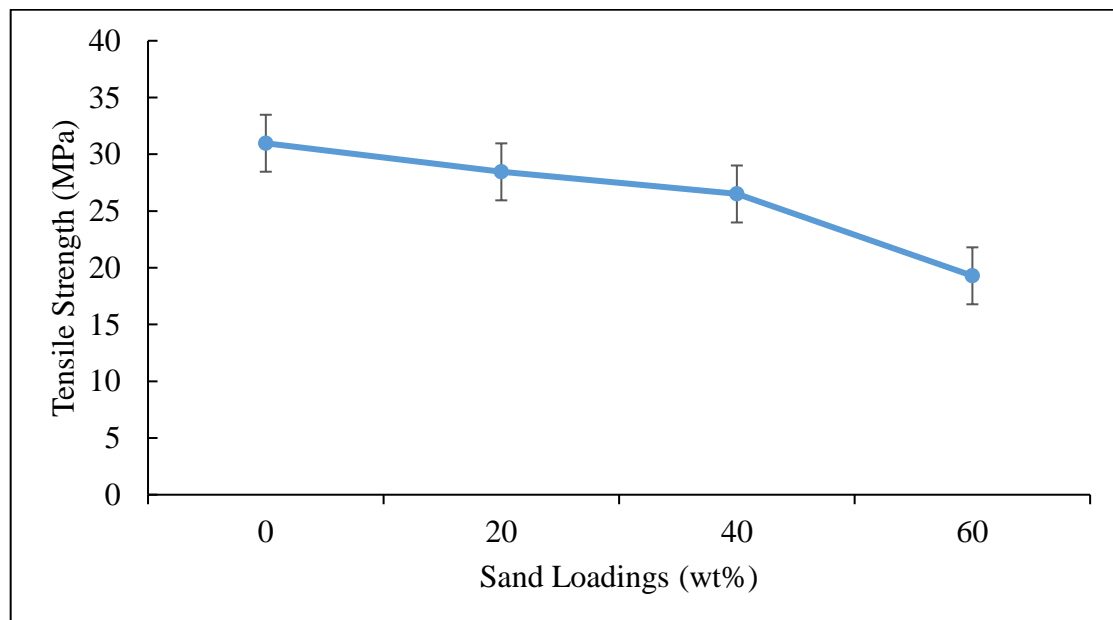


Figure 4.10: Tensile strength of HDPE-sand composites

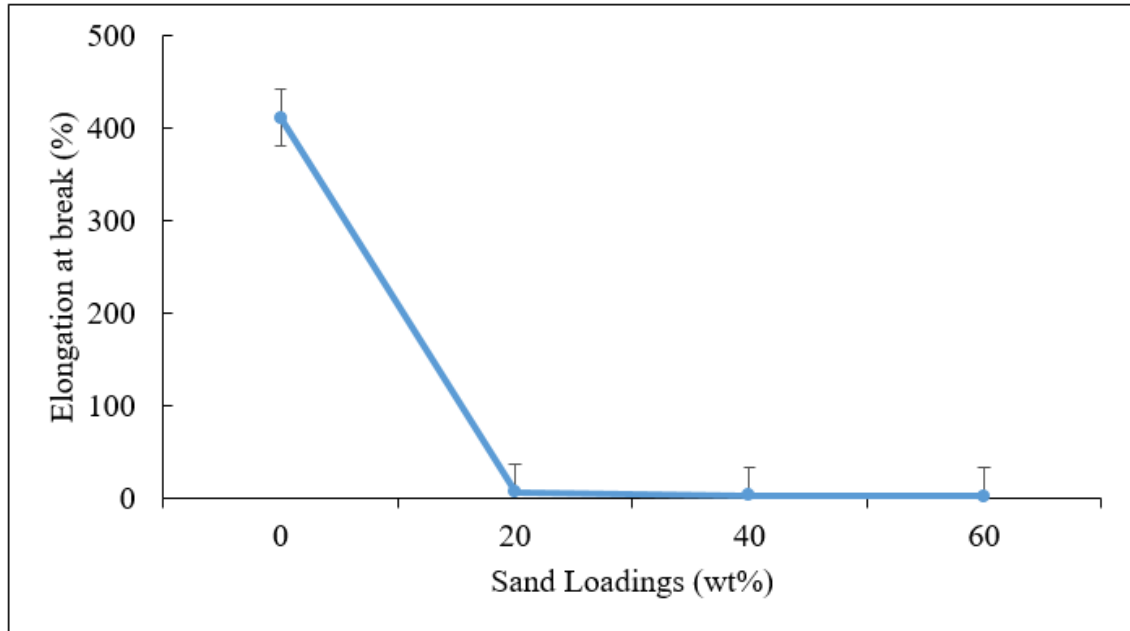


Figure 4.11: Elongation at break of HDPE-sand composites

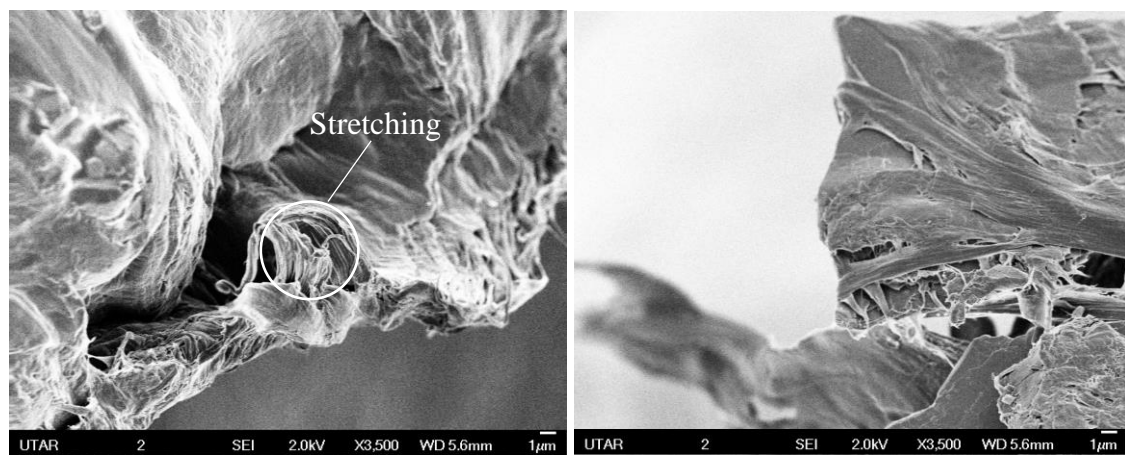
**Table 4.7: Mechanical Properties of HDPE and HDPE-sand composites**

<b>Sand Loadings (wt%)</b>	<b>Young's Modulus (Mpa)</b>	<b>Tensile Strength (Mpa)</b>	<b>Elongation at Break (%)</b>
<b>0</b>	930	30.97	410.57
<b>20</b>	1314	28.45	5.82
<b>40</b>	1509	26.50	2.45
<b>60</b>	1195	19.29	1.84

**Table 4.8: Comparison of tensile test results**

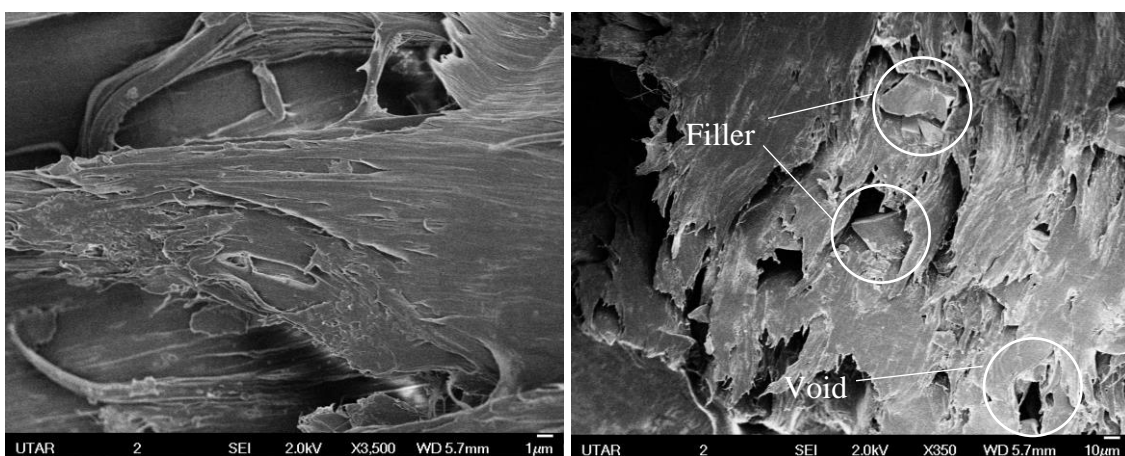
<b>Researched by</b>	<b>Composition</b>	<b>Young's Modulus (Mpa)</b>	<b>Tensile Strength (Mpa)</b>	<b>Elongation at Break (%)</b>
	HDPE/40wt% sand	(+62.25%) 1509	(-14.43%) 26.50	(-99%) 2.45
<b>(Cao et al., 2016)</b>	HDPE/10wt% peat ash	(+64.34%) 1276	(+8.78%) 32.44	Not Available
<b>(Igarza et al., 2014)</b>	PP/30wt% fly ash	(+24.87%) 2450	(-38.62%) 24.27	(-62.5%) 3.00
<b>(Lokuge and Aravinthan,2013)</b>	Polyester/20wt% fly ash	(+68.83%) 1300	(-45.45%) 6	Not Available

The fracture surface of HDPE and HDPE-sand composites after the tensile test were observed using FESEM to analyse the nature of the failure, Figure 4.2. For the neat HDPE, the elongation or stretching of the material can be found at the fracture side. At 20 and 40wt% filler loading, filler cannot be observe clearly at the fracture surface because it is well dispersed and no void was found. The fracture surfaces for both composites are more brittle without any matrix stretching. HDPE-sand composite with 60wt% sand loading shows excessive tearing of matrix, with fillers and voids observed on the surface. This indicates poor dispersion of filler in HDPE matrix at 60 wt% loading.



(a)

(b)



(c)

(d)

Figure 4.12: SEM Images of HDPE-sand composites with (a) neat HDPE (b) 20wt% sand (c) 40wt% sand at 3500X and (d) 60wt% sand at 350X

## CHAPTER 5

### CONCLUSION AND RECOMMENDATIONS

#### 5.1 Conclusion

HDPE-sand composites with high filler loading had been successfully fabricated by effective melt blending. Sand can be used as filler and the composite could be processed by melt blending method although the particle size is large and may form agglomeration. EDX result indicated the elementary component in the sand consisted of Si and O, in the form of  $\text{SiO}_2$ . PSA analysis showed that the particle size of sand is in average of  $33\mu\text{m}$ . Variety of alkanes and alkenes functional groups were found in the neat HDPE from FTIR. When the composite filler loading increased to 60wt%, the intensity of functional group for HDPE significantly reduce and become more similar with sand.  $T_m$  decreases as the filler loading increases while  $T_c$  was not affected by filler loading. Degree of crystallinity for composites at 20wt% sand loading is the highest. Besides, the stabilization torque for composites are lower than neat HDPE which mean it is easier to process in melt blending technique. MFI also indicate that 20wt% of sand loaded composites has the lowest viscosity and ease to flow. TGA curve show that the thermal decomposition temperature increases as filler loading increases. Mechanical performance of composites are tested by tensile test and the morphology was studied through SEM. Highest value of Young's modulus was obtained at 40 wt% filler loading which mean it is the stiffest among all.

Composites with 60wt% filler loading show brittle fracture surface with many voids and poor dispersion of filler in the matrix, 20 -40 wt% sand loading has the best morphology with good dispersion of filler and no void was found. Thus based on these results HDPE-sand composites has the potential to be developed as building construction material due to its ease of processing, high thermal decomposition durability and comparable tensile properties with others work.

## **5.2 Recommendation**

This study has indicated the enhancement of mechanical and physical properties of HDPE-sand composites. The promising development of HDPE-sand composites for construction sector has been proven. There are some steps that can be taken to optimize the process and properties of the HDPE-sand composites.

- Sand filler loading could be varied between 20 to 40wt% to find out the optimum loading for the HDPE-sand composite to maximize the mechanical and physical performance. Sand loading over 40wt% will cause the composites to become brittle.
- To study the mechanical properties of HDPE-sand composites better through impact and compression test.
- Coupling agent can be added into the mixing process to have better mixing properties and study the difference with or without coupling agent.

## REFERENCES

- Abee, R., Merex, D., Mee, M., Karlik, D., Guo, M. and Zou, D., 2014. *Thermally conductive and electrically insulative polymer compositions containing a thermally insulative filler and uses thereof*. US Patent 08741998B2.
- Adarsh, S., Manikanta, L. and Sha, S. (2016). Application of polymer composites in civil engineering. In: 3rd International Conference on Recent Trends in Engineering Science and Management. Bundi: Vendat College of Engineering and Technology.
- Aly, N. (2017). A review on utilization of textile composites in transportation towards sustainability. *IOP Conference Series: Materials Science and Engineering*, 254, pp. 242-250.
- Appiah, J.K., Boateng, V.N. and Tagbor, T.A., 2017. Use of waste plastic materials for road construction in Ghana. *Case Studies in Construction Materials*, 6, pp. 1-7.
- Badache, A., Benosman, A., Senhadji, Y. and Mouli, M. (2018). Thermo-physical and mechanical characteristics of sand-based lightweight composite mortars with recycled high-density polyethylene (HDPE). *Construction and Building Materials*, 163, pp.40-52.
- Barus, S., Zanetti, M., Bracco, P., Musso, S., Chiodoni, A. and Tagliaferro, A. (2010). Influence of MWCNT morphology on dispersion and thermal properties of polyethylene nanocomposites. *Polymer Degradation and Stability*, 95, pp.756-762.



- Bernier, M., Levy, G., Fine, P. and Borisover, M. (2013). Organic matter composition in soils irrigated with treated wastewater: FT-IR spectroscopic analysis of bulk soil samples. *Geoderma*, 209-210, pp.233-240.
- Bołtryk, M., Krupa, A. and Pawluczuk, E. (2018). Modification of the properties of the cement composites with the organic filler. *Construction and Building Materials*, 167, pp.143-153.
- Cao, Z., Daly, M., Geever, L., Major, I., Higginbotham, C. and Devine, D. (2016). Synthesis and characterization of high density polyethylene/peat ash composites. *Composites Part B: Engineering*, 94, pp.312-321.
- Ceresana, 2017. Market Study: Polyethylene - HDPE (4th ed.). Germany: Ceresana.
- Chandrasekaran, A., Rajalakshmi, A., Ravisankar, R. and Kalarasai, S. (2015). Analysis of beach rock samples of Andaman Island, India by spectroscopic techniques. *Egyptian Journal of Basic and Applied Sciences*, 2, pp.55-64.
- Chanhoun, M., Padonou, S., Adjovi, E., Olodo, E. and Doko, V. (2018). Study of the implementation of waste wood, plastics and polystyrenes for various applications in the building industry. *Construction and Building Materials*, 167, pp.936-941.
- Chantrasakul, S. and Amornsakchai, T. (2007). High strength polyethylene fibers from high density polyethylene/organoclay composites. *Polymer Engineering & Science*, 47, pp.943-950.
- CompositesLab. (2016). *History of Composites - Composites 101*. [online] Available at: <http://compositeslab.com/composites-101/history-of-composites/> [Accessed 4 Jan. 2018].

- Contat-Rodrigo, L., Ribes-Greus, A. and Imrie, C. (2002). Thermal analysis of high-density polyethylene and low-density polyethylene with enhanced biodegradability. *Journal of Applied Polymer Science*, 86, pp.764-772.
- Echeverria, C., Pahlevani, F., Gaikwad, V. and Sahajwalla, V. (2017). The effect of microstructure, filler load and surface adhesion of marine bio-fillers, in the performance of Hybrid Wood-Polypropylene Particulate Bio-composite. *Journal of Cleaner Production*, 154, pp.284-294.
- Ellerbrock, R. and Gerke, H. (2004). Characterizing organic matter of soil aggregate coatings and biopores by Fourier transform infrared spectroscopy. *European Journal of Soil Science*, 55(2), pp.219-228.
- Feng, J., Venna, S. and Hopkinson, D. (2016). Interactions at the interface of polymer matrix-filler particle composites. *Polymer*, 103, pp.189-195.
- Ferdous, W., Manalo, A., Aravinthan, T. and Van Erp, G. (2016). Properties of epoxy polymer concrete matrix: Effect of resin-to-filler ratio and determination of optimal mix for composite railway sleepers. *Construction and Building Materials*, 124, pp.287-300.
- Fioravante, V., Giretti, D. and Jamiolkowski, M. (2013). Small strain stiffness of carbonate Kenya Sand. *Engineering Geology*, 161, pp.65-80.
- Gabriel, L. H., 2010. History and Physical Chemistry of HDPE. *Chapter 1*. [online] Available at: [https://plasticpipe.org/pdf/chapter1history\\_physical\\_chemistry\\_hdpe.pdf](https://plasticpipe.org/pdf/chapter1history_physical_chemistry_hdpe.pdf) [Accessed 15 August 2017].
- Gao, J.L., Liu, Y.H., and Wei, S.D., 2011. Preparation and properties of High-density polyethylene/silica composites. *Advanced Materials Research*, 279, pp. 115-119.

- GoBrick (1992). *Brick Masonry Material Properties*. [online] Gobrick.com. Available at: <http://www.gobrick.com/portals/25/docs/technical%20notes/tn3a.pdf> [Accessed 17 Apr. 2018].
- González, C., Vilatela, J., Molina-Aldareguía, J., Lopes, C. and LLorca, J. (2017). Structural composites for multifunctional applications: Current challenges and future trends. *Progress in Materials Science*, 89, pp.194-251.
- Hamdhan, I.N. and Clarke, B.G., 2010. Determination of Thermal Conductivity of Coarse and Fine Sand Soils. In: *Proceedings World Geothermal Congress 2010. Bali, Indonesia, 25-29 April 2010*. Leeds, UK: Leeds University.
- Hanna, R. (1965). Infrared Absorption Spectrum of Silicon Dioxide. *Journal of the American Ceramic Society*, 48, pp.595-599.
- Huang, R., Xu, X., Lee, S., Zhang, Y., Kim, B. and Wu, Q. (2013). High Density Polyethylene Composites Reinforced with Hybrid Inorganic Fillers: Morphology, Mechanical and Thermal Expansion Performance. *Materials*, 6, pp.4122-4138.
- Humphreys, M.F. (2003). The use of polymer composites in construction. Queensland University Of Technology, Australia.
- Igarza, E., Pardo, S., Abad, M., Cano, J., Galante, M., Pettarin, V. and Bernal, C. (2014). Structure–fracture properties relationship for Polypropylene reinforced with fly ash with and without maleic anhydride functionalized isotactic Polypropylene as coupling agent. *Materials & Design*, 55, pp.85-92.
- Imai, Y., 2014. Encyclopedia of Polymeric Nanomaterials. Inorganic Nano-fillers for Polymers, pp. 1-7.

- Jo, B., Park, S. and Kim, D. (2008). Mechanical properties of nano-MMT reinforced polymer composite and polymer concrete. *Construction and Building Materials*, 22, pp.14-20.
- Johnson, T. (2017). *The Fascinating Story of Composite Plastic Materials*. [online] ThoughtCo. Available at: <https://www.thoughtco.com/history-of-composites-820404> [Accessed 5 Jan. 2018].
- Joseph, C. (2013). *What Is Sand?*. [online] Live Science. Available at: <https://www.livescience.com/34748-what-is-sand-beach-sand.html> [Accessed 3 Jan. 2018].
- Kelnar, I., Bal, Ü., Zhigunov, A., Kaprálková, L., Fortelný, I., Krejčíková, S. and Kredatusová, J. (2018). Complex effect of graphite nanoplatelets on performance of HDPE/PA66 microfibrillar composites. *Composites Part B: Engineering*, 144, pp.220-228.
- Kewalramani, M. (2014). Environmentally Sustainable Concrete Curing with Coloured Polythene Sheets. *APCBEE Procedia*, 9, pp.241-246.
- Kim, H., Biswas, J. and Choe, S. (2006). Effects of stearic acid coating on zeolite in LDPE, LLDPE, and HDPE composites. *Polymer*, 47, pp.3981-3992.
- Kulshreshtha, Y., Schlangen, E., Jonkers, H., Vardon, P. and van Paassen, L. (2017). CoRncrete: A corn starch based building material. *Construction and Building Materials*, 154, pp.411-423.
- Kumar, S. and Singh, R. (2011). Recovery of hydrocarbon liquid from waste high density polyethylene by thermal pyrolysis. *Brazilian Journal of Chemical Engineering*, 28, pp.659-667.

- Kumar, S. and Singh, R. (2015). Microbial degradation of low density polyethylene (LDPE): A review. *Journal of Environmental Chemical Engineering*, 3, pp.462-473.
- Kumar, S. and Singh, R. (2018). *Thermolysis of High-Density Polyethylene to Petroleum Products*.
- Ling, P., Ismail, H. and Bakar, A. (2016). Influence of Kenaf (KNF) Loading on Processing Torque and Water Absorption Properties of KNF-Filled Linear Low-Density Polyethylene/Poly (vinyl alcohol) (LLDPE/PVA) Composites. *Procedia Chemistry*, 19, pp.505-509.
- Lapčík, L., Maňas, D., Lapčíková, B., Vašina, M., Staněk, M., Čépe, K., Vlček, J., Waters, K., Greenwood, R. and Rowson, N. (2018). Effect of filler particle shape on plastic-elastic mechanical behavior of high density poly(ethylene)/mica and poly(ethylene)/wollastonite composites. *Composites Part B: Engineering*, 141, pp.92-99.
- Lokuge, W. and Aravinthan, T. (2013). Effect of fly ash on the behaviour of polymer concrete with different types of resin. *Materials & Design*, 51, pp.175-181.
- Manoharan, T., Laksmanan, D., Mylsamy, K., Sivakumar, P. and Sircar, A. (2018). Engineering properties of concrete with partial utilization of used foundry sand. *Waste Management*, 71, pp.454-460.
- Mathijssen, D. (2016). LEGO-like sand reinforced polyester bricks are set to revolutionize the building world. *Reinforced Plastics*, 60, pp.362-368.
- McIntosh, P. (2014). *Understanding Earth II: Testing earth*. [online] Natural Building Collective. Available at: <https://naturalbuildingcollective.wordpress.com/tag/tensile-strength/> [Accessed 20 April 2018].

- Mendez, O., 2016. *Uncovering the Revolutionary "Eco Blocks" From Conceptos Plasticos* [online] Available at: < <https://www.buildabroad.org/2016/08/18/eco-blocks/> > [Accessed 26 October 2017].
- Mohanty, S., Verma, S. and Nayak, S. (2006). Dynamic mechanical and thermal properties of MAPE treated jute/HDPE composites. *Composites Science and Technology*, 66(3-4), pp.538-547.
- Mosallam, A. (2014). Polymer Composites in Construction: An Overview. *SOJ Materials Science & Engineering*, 2, pp.01-25.
- Müller, C., Molinelli, A., Karlowatz, M., Aleksandrov, A., Orlando, T. and Mizaikoff, B. (2011). Infrared Attenuated Total Reflection Spectroscopy of Quartz and Silica Micro- and Nanoparticulate Films. *The Journal of Physical Chemistry C*, 116(1), pp.37-43.
- Patnayaka, R., 2013. BUILDING MATERIALS - SAND. [online] Available at: < <https://www.slideshare.net/rpdesigndesk/building-materials-sand> > [Accessed 21 August 2017].
- Pendhari, S., Kant, T. and Desai, Y. (2008). Application of polymer composites in civil construction: A general review. *Composite Structures*, 84, pp.114-124.
- Pérez, E., Pérez, C., Bernal, C., Greco, A. and Maffezzoli, A. (2015). Mechanical behavior of fibers and films based on PP/Quartz composites. *Polymer Composites*, 38, pp.1631-1639.
- Pešić, N., Živanović, S., Garcia, R. and Papastergiou, P. (2016). Mechanical properties of concrete reinforced with recycled HDPE plastic fibres. *Construction and Building Materials*, 115, pp.362-370.

- Philip Tice, 2003. Packaging Materials. *Polyethylene for Food Packaging Applications*. [online] Available at: <<http://ilsa.org/mexico/wp-content/uploads/sites/29/2016/09/Packaging-Materials-4-Polyethylene-for-Food-Packaging-Applications.pdf>> [Accessed 27 August 2017].
- Pickering, K., Efendy, M. and Le, T. (2016). A review of recent developments in natural fibre composites and their mechanical performance. *Composites Part A: Applied Science and Manufacturing*, 83, pp.98-112.
- Plastics Europe, 2016. *World Plastics Production 1950 – 2015*. [online] Available at: <<https://committee.iso.org/files/live/sites/tc61/files/The%20Plastic%20Industry%20Berlin%20Aug%202016%20-%20Copy.pdf>> [Accessed 21 August 2017].
- Professor Plastic, 2015. *High Density Polyethylene (HDPE): So Popular*. [online] Available at: <<https://www.plasticmakeitpossible.com/about-plastics/types-of-plastics/professor-plastic-high-density-polyethylene-hdpe-so-popular/>> [Accessed 21 August 2017].
- Roman, C. and García-Morales, M. (2018). Comparative assessment of the effect of micro- and nano- fillers on the microstructure and linear viscoelasticity of polyethylene-bitumen mastics. *Construction and Building Materials*, 169, pp.83-92.
- Ryan, V., 2008. *Properties of HDPE- High density polyethylene*. [online] Available at: <<http://www.technologystudent.com/rmprep08/prophd1.html>> [Accessed 24 October 2017].
- Sarasini, F., Tirillò, J., Sergi, C., Seghini, M., Cozzarini, L. and Graupner, N. (2018). Effect of basalt fibre hybridisation and sizing removal on mechanical and thermal properties of hemp fibre reinforced HDPE composites. *Composite Structures*, 188, pp.394-406.

- Shao, Y., Yang, Z., Deng, B., Yin, B. and Yang, M. (2018). Tuning PVDF/PS/HDPE polymer blends to tri-continuous morphology by grafted copolymers as the compatibilizers. *Polymer*, 140, pp.188-197.
- Shin, J. and Selke, E.M. (2014). Food packaging. *Food processing: principles and applications*. pp 249–273
- Soliman, N. and Tagnit-Hamou, A. (2017). Using glass sand as an alternative for quartz sand in UHPC. *Construction and Building Materials*, 145, pp.243-252.
- Subaşı, S., Öztürk, H. and Emiroğlu, M. (2017). Utilizing of waste ceramic powders as filler material in self-consolidating concrete. *Construction and Building Materials*, 149, pp.567-574.
- Tsou, A. and Waddell, W. (2004). Fillers. *Encyclopedia of Polymer Science and Technology*.
- UKEssays, (2013). Various disadvantages of steel. [online]. Available from: <http://www.ukessays.com/essays/construction/various-disadvantages-of-steel.php?vref=1> [Accessed 7 April 2018].
- Verbeek, C. and du Plessis, B. (2005). Density and flexural strength of phosphogypsum–polymer composites. *Construction and Building Materials*, 19, pp.265-274.
- Wang, G., Yu, D., Kelkar, A. and Zhang, L. (2017). Electrospun nanofiber: Emerging reinforcing filler in polymer matrix composite materials. *Progress in Polymer Science*, 75, pp.73-107.
- Wang, J., Ling, H. and Mohri, Y. (2007). Stress-Strain Behavior of a Compacted Sand-Clay Mixture. *Soil Stress-Strain Behavior: Measurement, Modeling and Analysis*, pp.491-502.



Wang, R.M., Zheng, S.R. and Zheng, Y.P., 2011. *Polymer Matrix Composites and Technology*. Cambridge: Woodhead Publishing.

Whisnant, 2000. *Polymer Chemistry, Topology*. [online] Available at: <<https://faculty.uscupstate.edu/llever/polymer%20resources/Topology.htm>> [Accessed 21 August 2017].

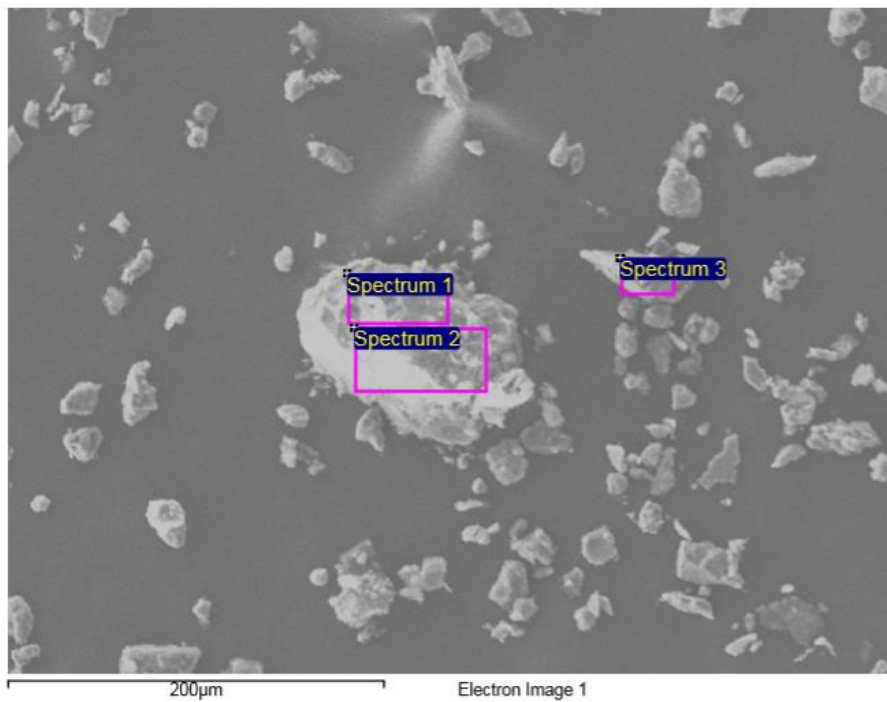
Wong, V. (2006). *Inspirational chemistry*. London: Royal Society of Chemistry, pp.113-128.

Zeepe Construction, 2015. HDPE Pipe (High Density Polyethylene Pipe). [online] Available at: <<http://www.zeepeconstruction.com/products/hdpe-pipe/>> [Accessed 21 August 2017].

## APPENDICES

### APPENDIX A: Energy-dispersive X-ray spectroscopy

(a) EDX Spectrum Summary for Sand Filler



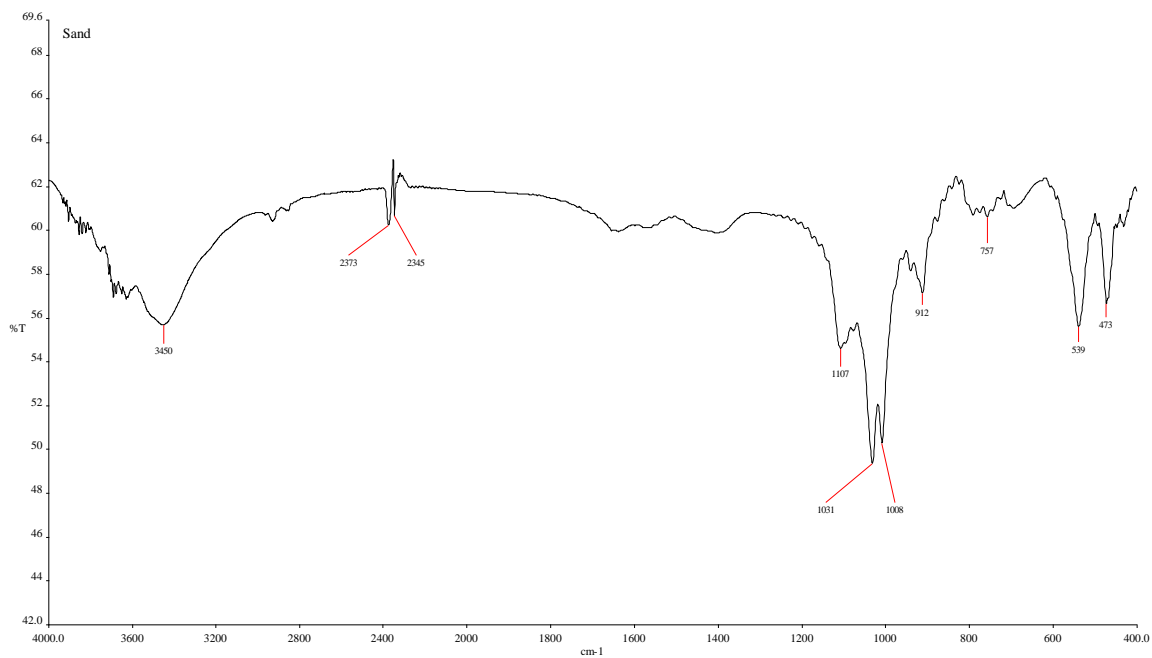
Processing option : All elements analysed (Normalised)

Spectrum	In stats.	C	O	Al	Si	K	Ca	Cu	Mo	Total
Spectrum 1	Yes	19.16	58.08	1.99	20.41	0.09		0.26		100.00
Spectrum 2	Yes	22.74	53.45	2.28	21.53					100.00
Spectrum 3	Yes	28.85	53.01	2.36	14.95	0.11	0.13	0.26	0.34	100.00
Max.		28.85	58.08	2.36	21.53	0.11	0.13	0.26	0.34	
Min.		19.16	53.01	1.99	14.95	0.09	0.13	0.26	0.34	

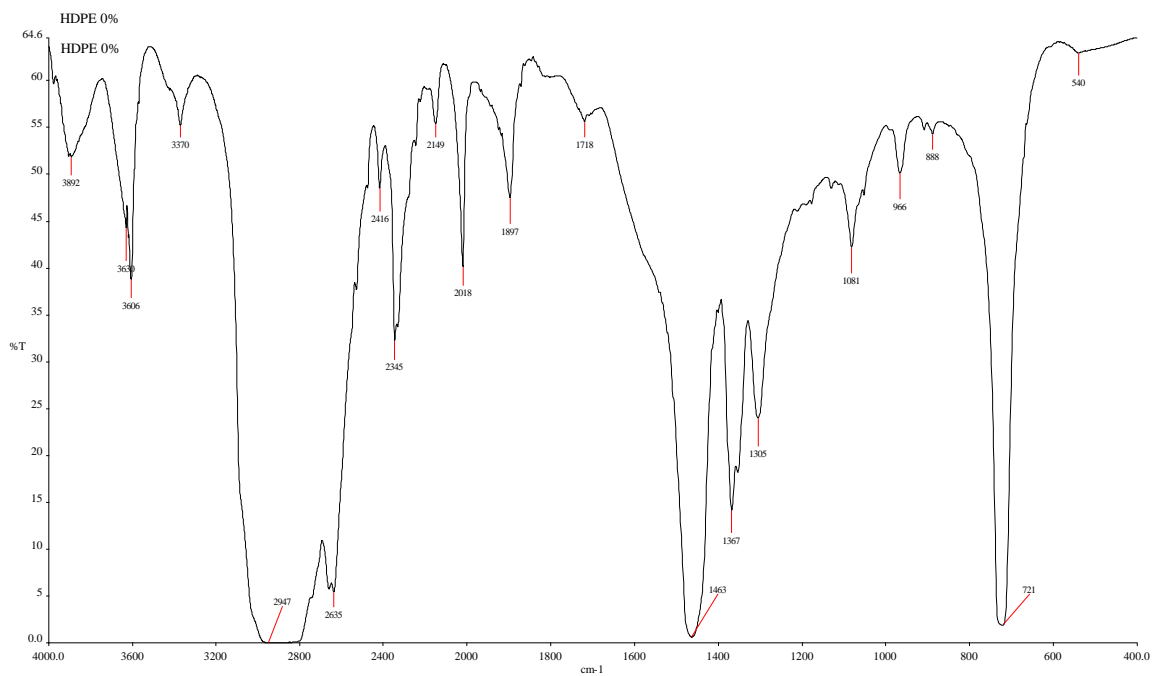
All results in weight%

**APPENDIX B: Fourier Transform Infrared Spectroscopy**

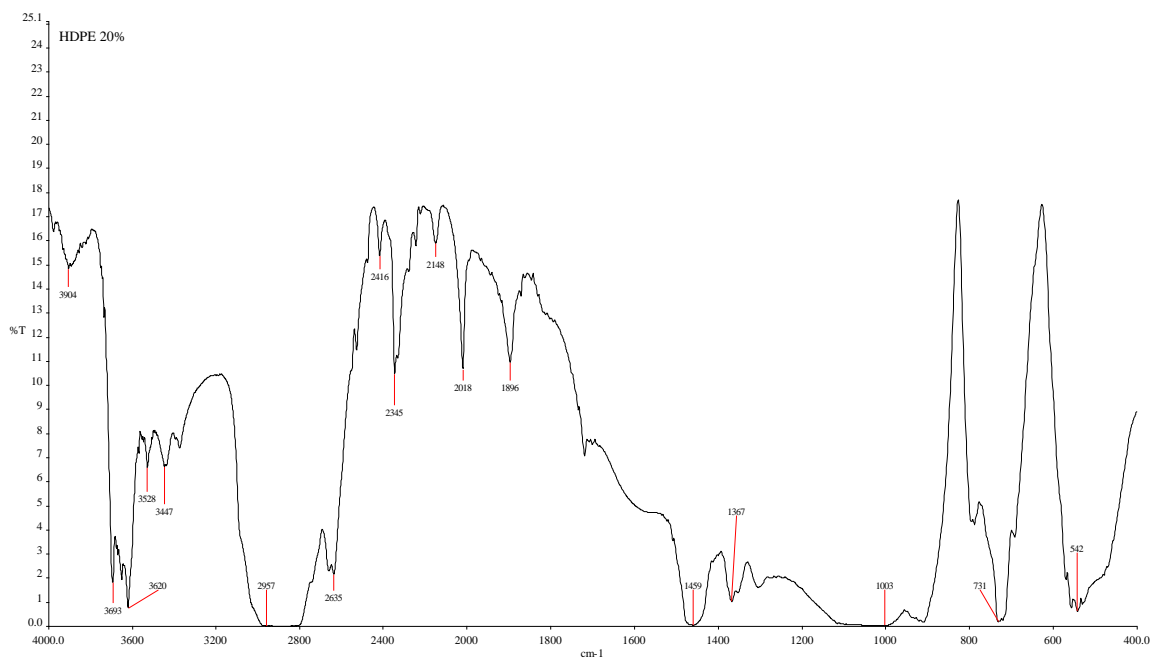
(a) Sand



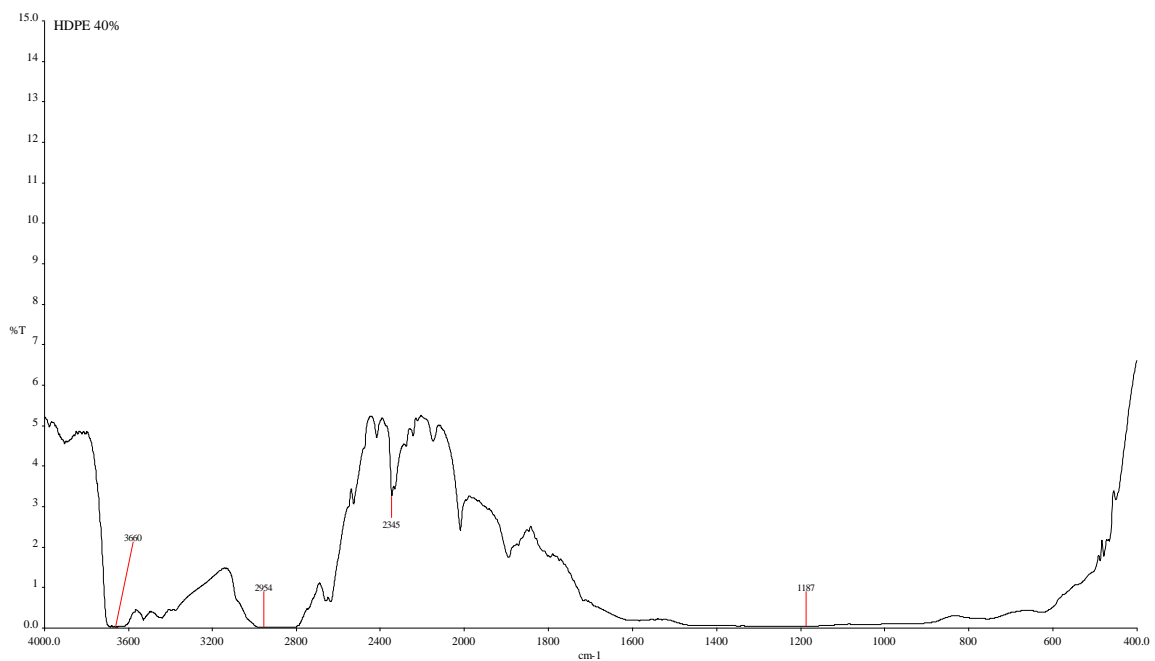
(b) Neat HDPE



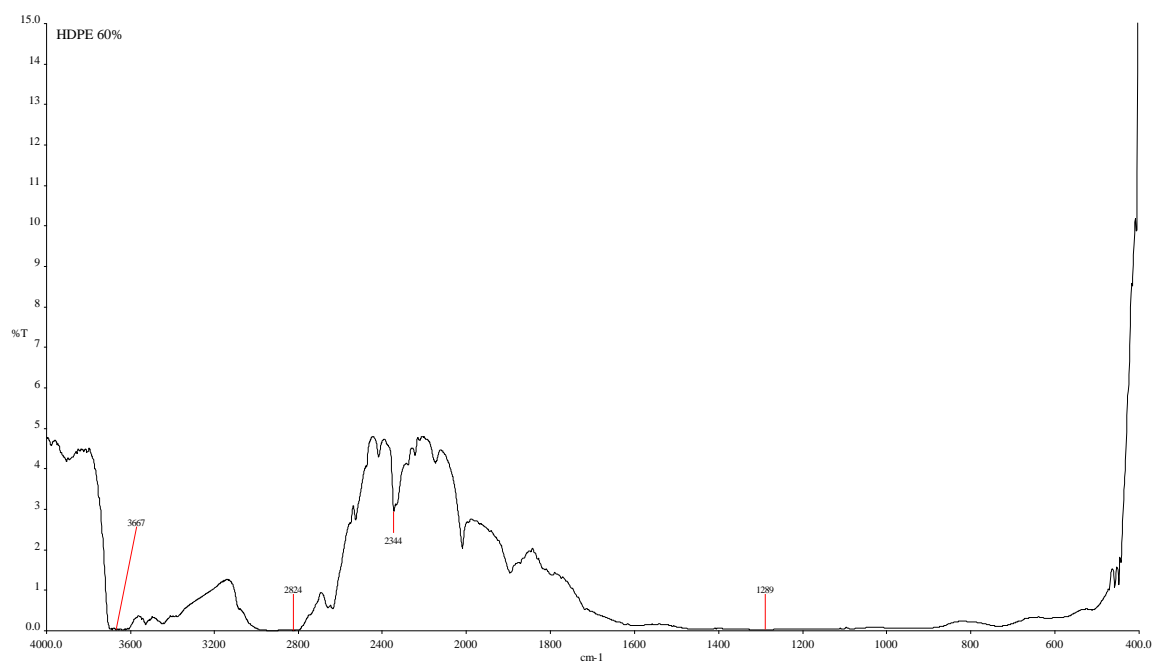
(c) HDPE/20wt% Sand



(d) HDPE/40wt% Sand

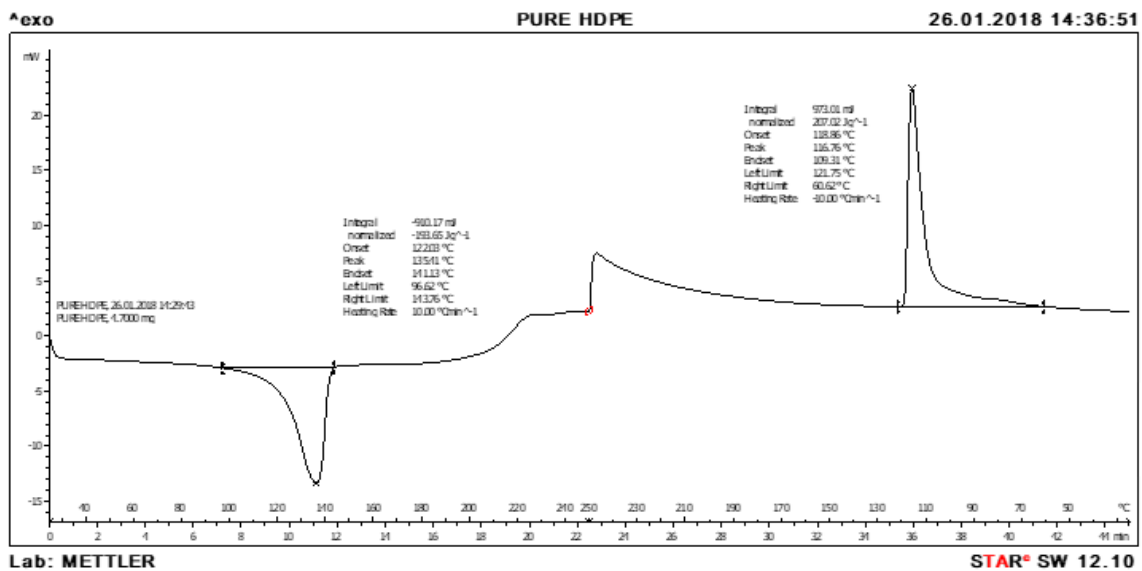


(d) HDPE/60wt% Sand

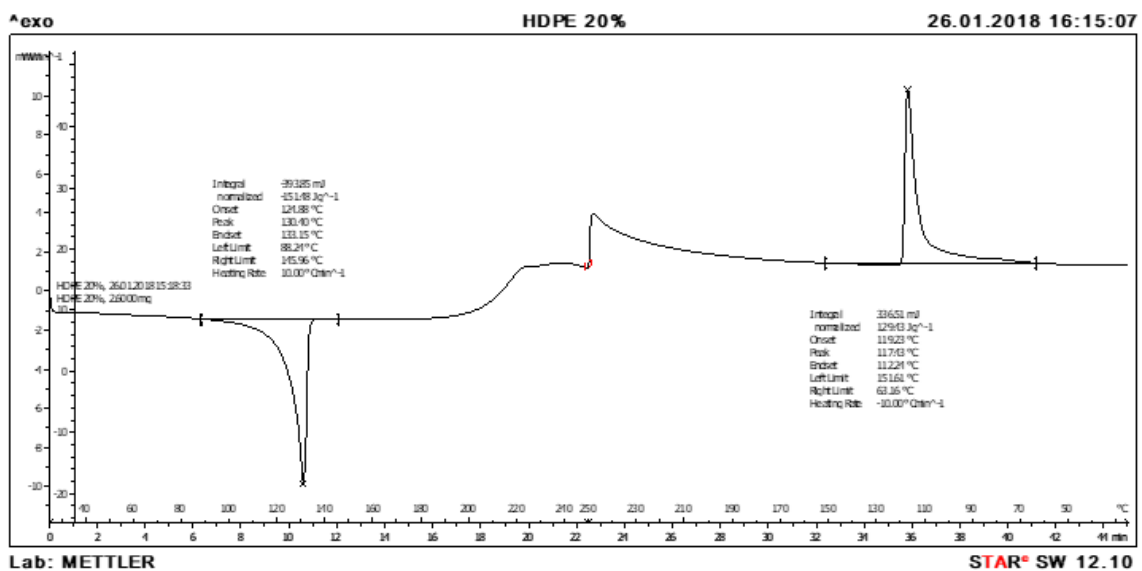


## APPENDIX C: Differential Scanning Calorimetry

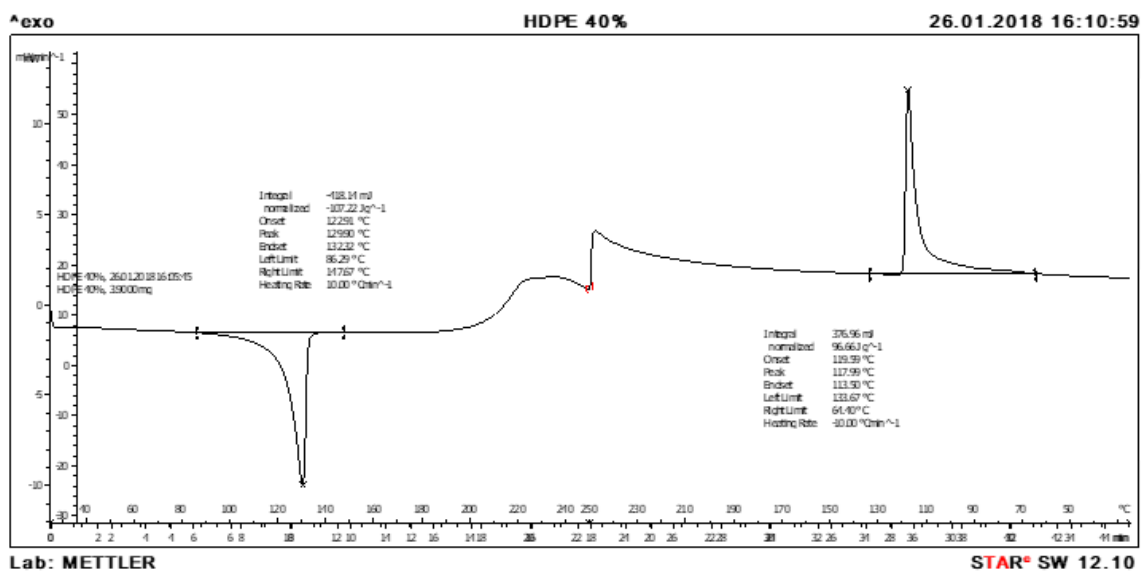
(a) Neat HDPE



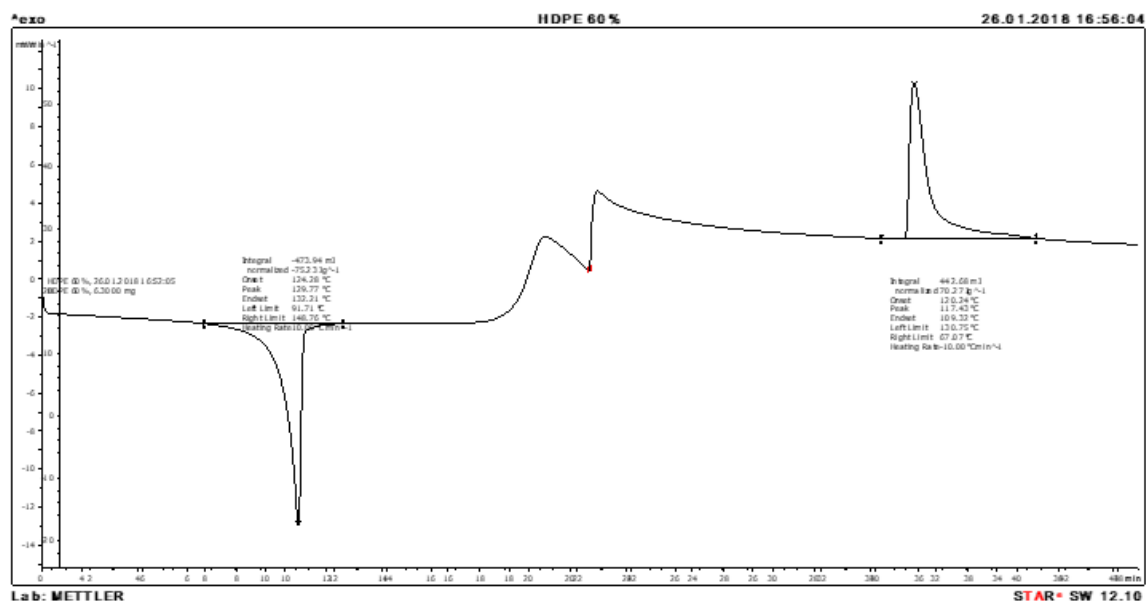
(b) HDPE/20wt% Sand



(c) HDPE/40wt% Sand

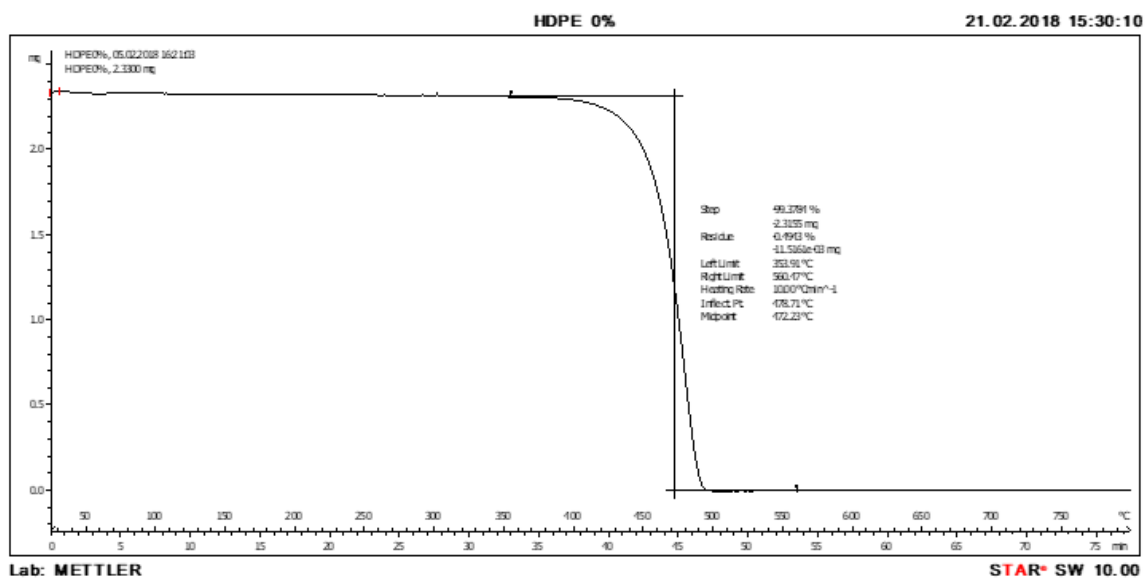


(d) HDPE/60wt% Sand

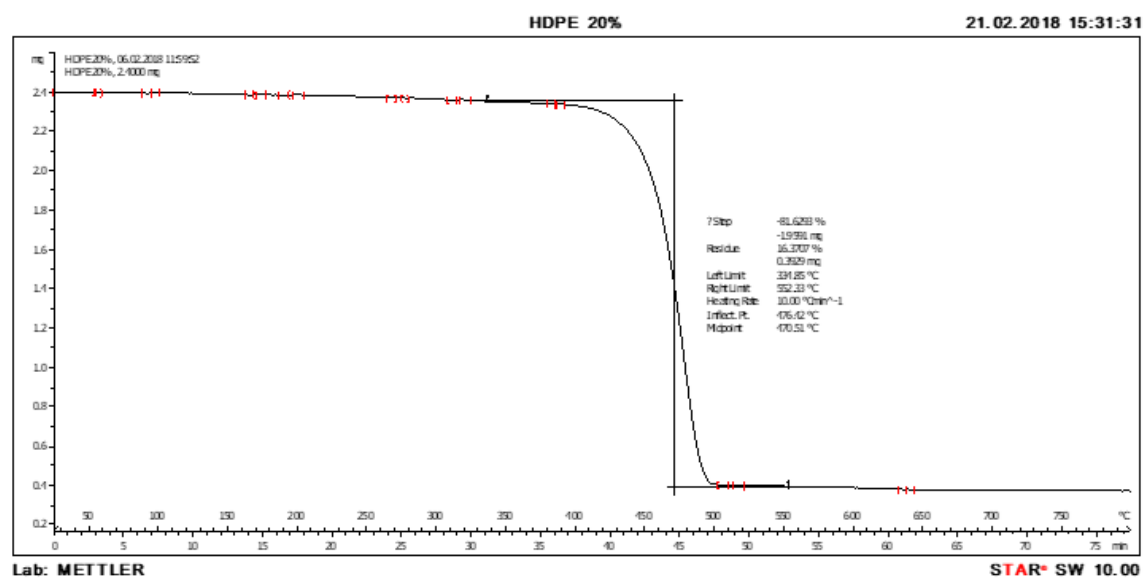


## APPENDIX D: Thermal Gravimetric Analysis

(a) Neat HDPE

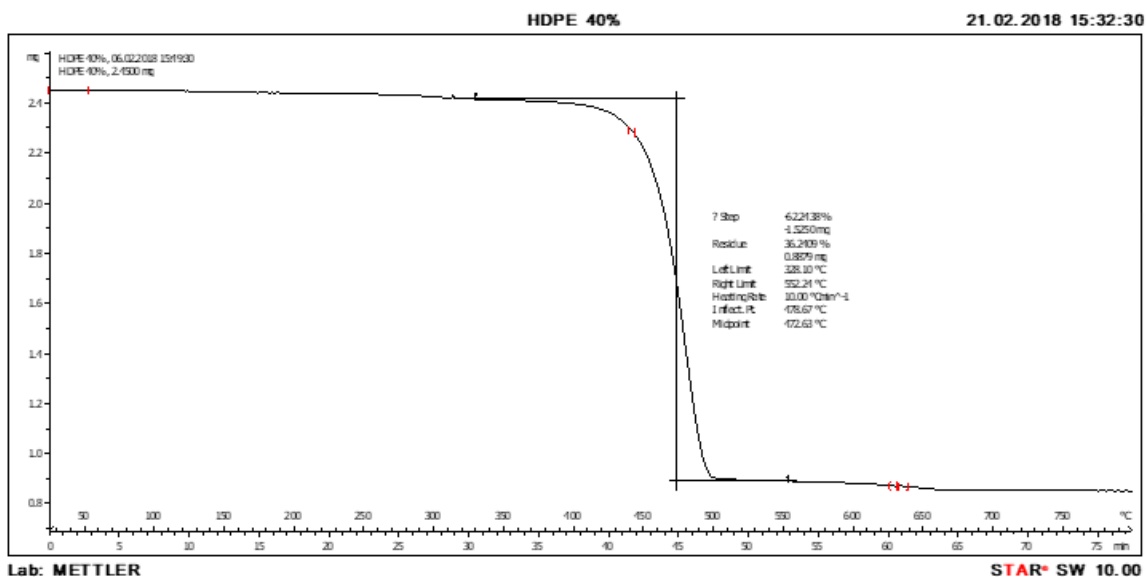


(b) HDPE/20wt% Sand

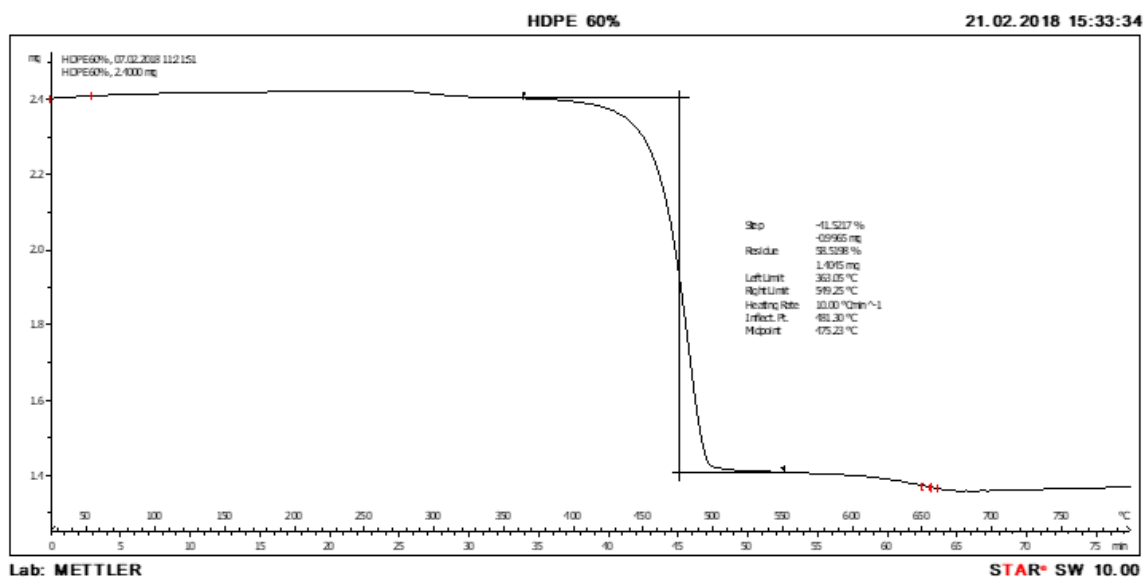




(c) HDPE/40wt% Sand



(d) HDPE/60wt% Sand



## APPENDIX E: Particle Size Analysis Report

**Complete** *Thank you for using PDF Complete.*

[Click Here to upgrade to Unlimited Pages and Expanded Features](#)

### Analysis Report

**Measured:**  
Friday, 27 October, 2017 1:50:35 PM

**Analysed:**  
Friday, 27 October, 2017 1:50:37 PM

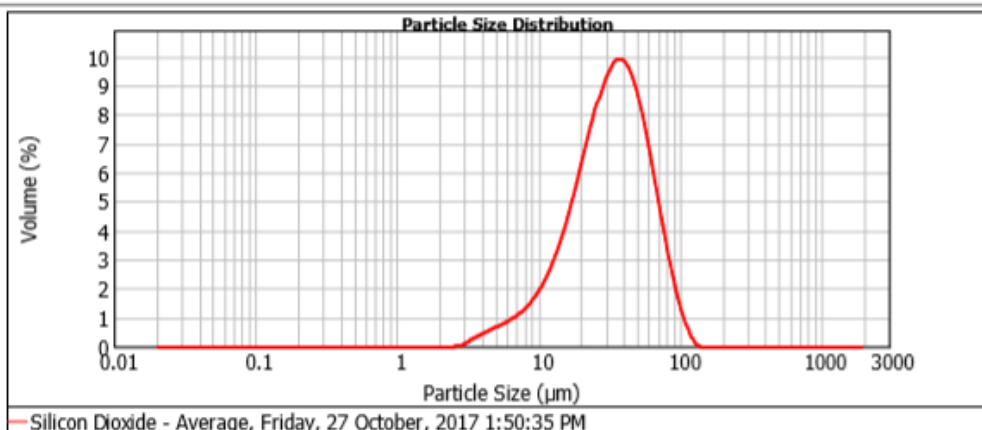
**Sample Source & type:** Measured by: User

**Sample bulk lot ref:** Result Source: Averaged

<b>Particle Name:</b> Silica Dioxide	<b>Accessory Name:</b> Hydro 2000MU (A)	<b>Analysis model:</b> General purpose	<b>Sensitivity:</b> Enhanced
<b>Particle RI:</b> 1.450	<b>Absorption:</b> 0	<b>Size range:</b> 0.020 to 2000.000 um	<b>Obscuration:</b> 11.96 %
<b>Dispersant Name:</b> Water	<b>Dispersant RI:</b> 1.330	<b>Weighted Residual:</b> 0.880 %	<b>Result Emulation:</b> Off

<b>Concentration:</b> 0.0399 %Vol	<b>Span :</b> 1.645	<b>Uniformity:</b> 0.51	<b>Result units:</b> Volume
<b>Specific Surface Area:</b> 0.253 m <sup>2</sup> /g	<b>Surface Weighted Mean D[3,2]:</b> 23.671 um	<b>Vol. Weighted Mean D[4,3]:</b> 36.933 um	

**d(0.1): 12.557 um                      d(0.5): 32.973 um                      d(0.9): 66.809 um**



Size (µm)	Volume In %	Size (µm)	Volume In %	Size (µm)	Volume In %	Size (µm)	Volume In %	Size (µm)	Volume In %	Size (µm)	Volume In %
0.010	0.00	0.105	0.00	1.006	0.00	11.482	2.47	120.226	0.11	1258.925	0.00
0.011	0.00	0.120	0.00	1.259	0.00	13.183	3.18	138.038	0.00	1445.440	0.00
0.013	0.00	0.138	0.00	1.445	0.00	15.136	4.03	158.489	0.00	1659.587	0.00
0.015	0.00	0.158	0.00	1.660	0.00	17.378	5.03	181.970	0.00	1905.461	0.00
0.017	0.00	0.182	0.00	1.905	0.00	19.953	6.10	208.930	0.00	2187.762	0.00
0.020	0.00	0.209	0.00	2.188	0.00	22.909	7.16	239.883	0.00	2511.886	0.00
0.023	0.00	0.240	0.00	2.512	0.01	26.303	8.07	275.423	0.00	2894.032	0.00
0.026	0.00	0.275	0.00	2.884	0.12	30.200	8.72	316.228	0.00	3311.311	0.00
0.030	0.00	0.316	0.00	3.311	0.29	34.674	8.96	363.078	0.00	3801.894	0.00
0.035	0.00	0.363	0.00	3.802	0.41	39.811	8.73	416.889	0.00	4365.158	0.00
0.040	0.00	0.417	0.00	4.365	0.55	45.709	8.00	478.630	0.00	5011.872	0.00
0.046	0.00	0.479	0.00	5.012	0.67	52.481	6.87	549.541	0.00	5754.399	0.00
0.052	0.00	0.550	0.00	5.754	0.81	60.256	5.46	630.957	0.00	6608.934	0.00
0.060	0.00	0.631	0.00	6.607	0.98	69.183	3.98	724.436	0.00	7585.776	0.00
0.069	0.00	0.724	0.00	7.586	1.20	79.433	2.59	831.764	0.00	8709.636	0.00
0.079	0.00	0.832	0.00	8.710	1.51	91.201	1.45	964.993	0.00	10000.000	0.00
0.091	0.00	0.955	0.00	10.000	1.92	104.713	0.63	1096.478	0.00		
0.105	0.00	1.096	0.00	11.482		120.226		1258.925	0.00		

